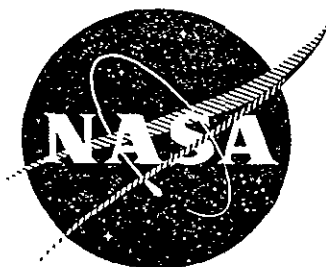


R77AEG190

NASA CR 151958



THRUST REVERSER DESIGN STUDIES FOR AN OVER-THE-WING STOL TRANSPORT

by

R.C. AMMER and H.D. SOWERS

GENERAL ELECTRIC COMPANY

(NASA-CR-151958), THRUST REVERSER DESIGN STUDIES FOR AN OVER-THE-WING STOL TRANSPORT (General Electric Co.) 67 p HC A04/MF A01 CSCS 21E	N77-19071 Unclas 22677 G3/07
--	---------------------------------------

Prepared For

National Aeronautics and Space Administration

NASA *Ames* Research Center
Contract NAS2-9254

**ORIGINAL PAGE IS
OF POOR QUALITY**

1. Report No. NASA CR-151958		2. Government Accession No.		3. Recipient's Catalog No.	
4. Title and Subtitle Thrust Reverser Design Studies for an Over-the-Wing STOL Transport				5. Report Date March 1977	
				6. Performing Organization Code	
7. Author(s) R.C. Ammer and H.D. Sowers				8. Performing Organization Report No. R77AEG190	
9. Performing Organization Name and Address General Electric Company Aircraft Engine Group, AE&TPD Cincinnati, Ohio 45215				10. Work Unit No.	
				11. Contract or Grant No. NAS2-9254	
12. Sponsoring Agency Name and Address National Aeronautics and Space Administration Washington, D.C. 20546				13. Type of Report and Period Covered Contract Report	
				14. Sponsoring Agency Code	
15. Supplementary Notes Study Report NASA Technical Representative: M.D. Falarski NASA-Ames Research Center, Moffett Field, Calif. 94035					
16. Abstract Aerodynamic and acoustics analytical studies were conducted to evaluate three thrust reverser design for potential use on commercial over-the-wing STOL transports. The concepts were: <ul style="list-style-type: none">• Integral D nozzle/target reverser• Integral D nozzle/top arc cascade reverser• Post exit target reverser integral with wing. Aerodynamic flowpaths and kinematic arrangements for each concept were established to provide a 50% thrust reversal capability. Analytical aircraft stopping distance/noise trade studies conducted concurrently with flowpath design have shown that these high efficiency reverser concepts can be employed at substantially reduced power settings to meet noise goals of 100 PNdB on a 152.4 m (500 ft) sideline and still meet 609.6 m (2000 ft) landing runway length requirements. From an overall installation standpoint, only the integral D nozzle/target reverser concept was found to penalize nacelle cruise performance (2-3% of net thrust); for this concept a larger nacelle diameter was required to match engine cycle effective area demand in reverse thrust. The most attractive reverser concept which emerged from this study was the top arc cascade reverser. Its selection was based on estimated aerodynamic and acoustic performance, and a qualitative assessment of relative mechanical complexity, weight and ultimate production manufacturing cost, considering wing structural design aspects of integrating the post exit target reverser concept into the wing. A scale model flowpath was also defined for application in reverser aerodynamic and acoustics research programs to be conducted by the NASA-Ames Flight Systems Research Division.					
17. Key Words (Suggested by Author(s)) Commercial STOL transport Aerodynamics Over-the-Wing Acoustics Nozzle Reverser Noise Reverser Target Cascade				18. Distribution Statement	
19. Security Classif. (of this report) Unclassified		20. Security Classif. (of this page) Unclassified		21. No. of Pages 61	22. Price*

* For sale by the National Technical Information Service, Springfield, Virginia 22151

TABLE OF CONTENTS

<u>Section</u>		<u>Page</u>
1.0	INTRODUCTION	1
2.0	SUMMARY	2
3.0	THRUST REVERSER CONCEPTUAL DESIGN STUDIES (TASK I)	4
3.1	Ground Rules	4
3.2	OTW STOL Transport Configuration	4
3.3	Engine Cycle Selection	6
3.4	Baseline Nacelle/Nozzle Configuration	8
3.5	Landing Distance Studies	13
3.6	Thrust Reverser Conceptual Design	15
3.6.1	Integral D Nozzle/Single Blocker Target Reverser	16
3.6.2	Integral D Nozzle/Top Arc Cascade Reverser Concept	25
3.6.3	Post Exit Target Reverser Integral With Wing	35
3.6.4	Effect of Aircraft Size	42
3.7	Concept Selection for Model Design (Task II)	42
4.0	APPLICATION OF REVERSER CONCEPT TO SCALE MODEL DESIGN (TASK II)	48
4.1	Scale Model Duct Design	48
4.2	Scale Model Reverser Design	52
4.2.1	Aerodynamic Flowpath	52
4.2.2	Cascade Vane Design	54
4.3	Scale Model Noise Estimates	54
5.0	NOMENCLATURE	59
6.0	REFERENCES	61

LIST OF ILLUSTRATIONS

<u>Figure</u>		<u>Page</u>
1.	OTW STOL Transport Top Arc Cascade Reverser Installation.	3
2.	STOL Aircraft Noise Goals	5
3.	OTW STOL Transport Engine Installation.	7
4.	Takeoff Noise Constituents.	9
5.	OTW STOL Transport Baseline Nacelle/Nozzle Configuration.	11
6.	Landing Distance Parametric Study.	14
7.	Integral D Nozzle and Target Reverser.	17
8.	Target Reverser Performance.	20
9.	Integral Target Reverse Thrust Noise.	22
10.	Engine Noise Constituents in Reverse Thrust.	23
11.	Total System Reverse Thrust Noise With Integral Target.	24
12.	Integral Target Reverse Thrust Spectra.	26
13.	Integral D Nozzle and Top Arc Cascade Reverser.	27
14.	Top Arc Cascade Reverser Area Sizing Study.	29
15.	Top Arc Cascade Thrust Reverser Parametric Performance.	30
16.	Cascade Reverse Thrust Noise.	32
17.	Total System Reverse Thrust Noise With Cascade.	33
18.	Cascade Reverse Thrust Spectra.	34
19.	Post Exit Target Reverser.	36
20.	Post Exit Target Reverser Performance.	37
21.	Post Exit Target Reverse Thrust Noise.	39

LIST OF ILLUSTRATIONS (Concluded)

<u>Figure</u>		<u>Page</u>
22.	Total System Reverse Thrust Noise With Post Exit Target.	40
23.	Post Exit Target Reverse Thrust Spectra.	41
24.	Effect of Aircraft Gross Weight on Reverse Thrust Noise.	43
25.	NASA-Ames Static Test Facility Schematic.	49
26.	Scale Model Forward Flowpath Design.	50
27.	Scale Model Exhaust Duct Cross-Sectional Area Distribution.	51
28.	Scale Model Reverser Flowpath Design.	53
29.	Cascade Vane Geometry.	55
30.	Predicted Scale Model Cascade Reverse Thrust OASPL.	57
31.	Predicted Scale Model Cascade Thrust Reverser Spectra.	58

LIST OF TABLES

<u>Table</u>		<u>Page</u>
I	Comparison of Conceptual Target Reverser Geometric Parameters With Reference Configuration.	19
II	Summary of Reverse Thrust Obtainable Within Noise Goal Limit.	45
III	OTW STOL Transport Reverser Concept Comparison.	46
IV	Top Arc Cascade Reverser Geometry and Performance Parameters.	47

1.0 INTRODUCTION

Commercial transports are equipped with some type of thrust reverser to reduce tire and brake wear during normal usage, and to limit landing ground roll in emergency situations such as icy runways or failed brake conditions. This will also be the case for turbofan-powered STOL transports. One type of STOL design which has received much attention because of its potentially simple and efficient design is the over-the-wing (OTW) propulsive lift concept.. Extensive research has been conducted to develop an OTW transport propulsion system which is quiet and efficient during takeoff and landing as well as cruise, while little research has been accomplished to develop an effective thrust reverser for the OTW system which will not exceed the low noise requirements of 609.6 m (2000 ft) runway STOL transports.

The General Electric Company, under contract to the NASA - Ames Research Center, has completed an aerodynamics and acoustics analytical study program to define the aerodynamic flowpath for a quiet, efficient OTW transport thrust reverser conceptual design. The study included installation of the conceptual reverser design into D shaped exhaust systems utilized for propulsive lift, and the application of the selected reverser concept to a scale model flowpath for use in experimental research by the NASA - Ames Large-Scale Aerodynamics Branch of the Flight Systems Research Division.

2.0 SUMMARY

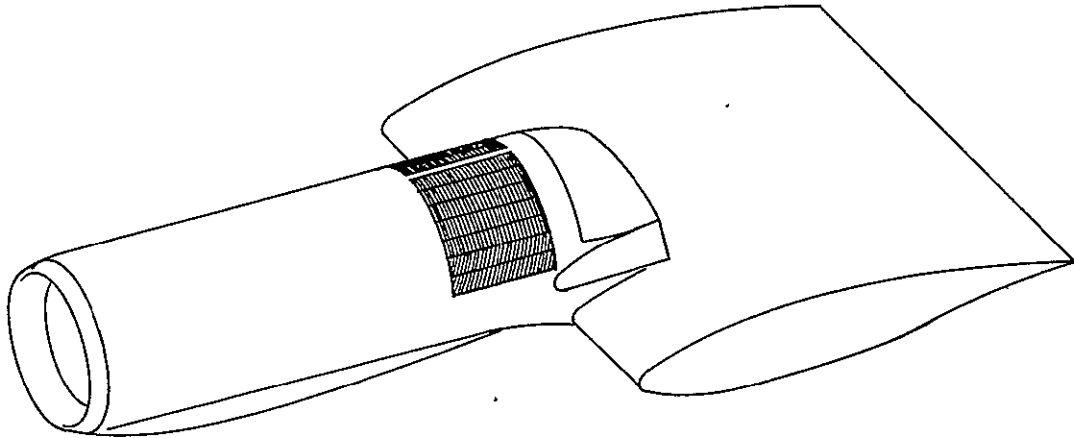
Aerodynamic and acoustics analytical studies were conducted to evaluate three thrust reverser design concepts for potential use on commercial over-the-wing STOL transports. The concepts were:

- Integral D nozzle/target reverser
- Integral D nozzle/top arc cascade reverser
- D nozzle post exit target reverser integral with wing.

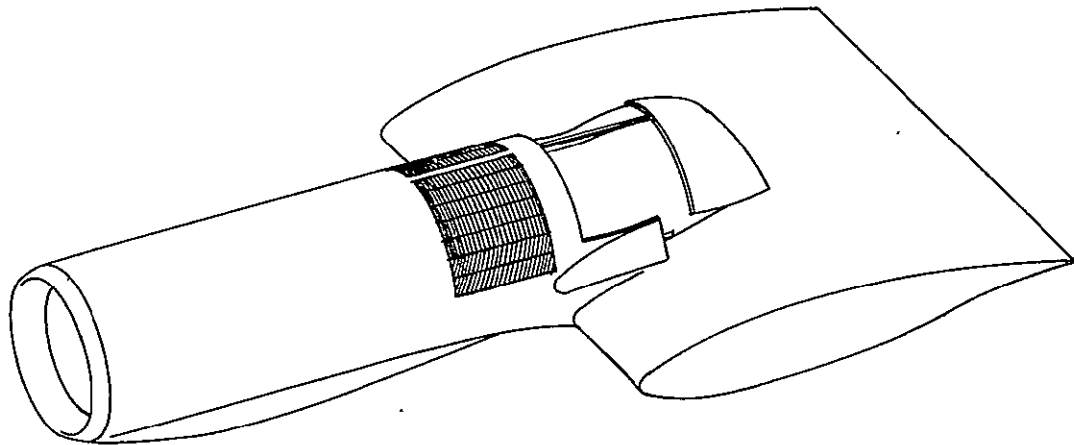
In Task I of this effort, aerodynamic flowpaths and kinematic arrangements for each concept were established to provide a 50% thrust reversal capability. Aircraft stopping distance and noise trade studies conducted concurrently with flowpath design have shown that these high efficiency reverser concepts can be employed at substantially reduced power settings to meet noise goals of 100 PNdB on a 152.4 m (500 ft) sideline and still meet 609.6 m (2000 ft) landing runway length requirements. From an overall installation standpoint, only the integral D nozzle/target reverser concept was found to penalize nacelle cruise performance (2-3% of engine cruise net thrust). For this concept a larger nacelle diameter was required to match engine cycle effective area demand in reverse thrust.

The most attractive reverser concept which emerged from this study was the top arc reverser design shown in Figure 1. Its selection was based on acceptable aero/acoustic performance and a qualitative assessment of relative mechanical complexity, weight and ultimate production manufacturing cost, with consideration for wing structural design aspects of integrating the post exit target reverser concept into the wing.

In Task II, a scale model flowpath for the top arc cascade reverser was defined for aerodynamic and acoustics research programs to be conducted by the NASA - Ames Flight Systems Research Division.



Cruise Flight



Reverse Thrust

Figure 1 OTW STOL Transport Top Arc Cascade Reverser Installation.

3.0 THRUST REVERSER CONCEPTUAL DESIGN STUDIES (TASK I)

3.1 GROUND RULES

Thrust reverser conceptual design analytical studies were conducted for a commercial over-the-wing (OTW) STOL transport in the 45,356 kg (100,000 lb) to 113,391 kg (250,000 lb) gross weight range. The aircraft was assumed to be powered by high-bypass ratio, mixed flow, turbofan engines having D-shaped nozzles for propulsive lift enhancement. The aircraft was required to operate from 609.6 m (2000 ft) runways. The conceptual design of the thrust reverser was to provide at least 50% reversal (reverse thrust divided by forward thrust at the same engine operating condition). Installation of the reverser system was not to compromise aircraft performance during takeoff, landing and cruise.

Noise goals were selected for takeoff, approach and reverse thrust. The first two goals help to establish the cycle and nacelle suppression requirements for the study engine configurations. The commercial STOL requirements, as shown in Figure 2, are 95 EPNdB on a 152.4 m (500 ft) sideline in both the take-off and approach modes. This requirement should also apply during the reverse thrust mode of operation. Evaluating reverser noise in EPNdB is difficult, however, due to the many variables which are changing as the reverser is applied, such as engine power setting, aircraft speed, and directivity of the noise sources. All of these must be evaluated in PNdB as a function of time, then a duration correction applied to obtain EPNdB. Since the time the reverser is used is relatively short, the correction from PNdB to EPNdB is negative, i.e., EPNdB is less than maximum PNdB. For purposes of evaluation, a reverse thrust noise goal of 100 PNdB on a 152.4 m (500 ft) sideline was established which is comparable to a take-off and approach goal of 95 EPNdB.

3.2 OTW STOL TRANSPORT CONFIGURATION

The conceptual STOL transport configuration selected for these studies is a four-engine aircraft with over-the-wing nacelle placement. An aircraft

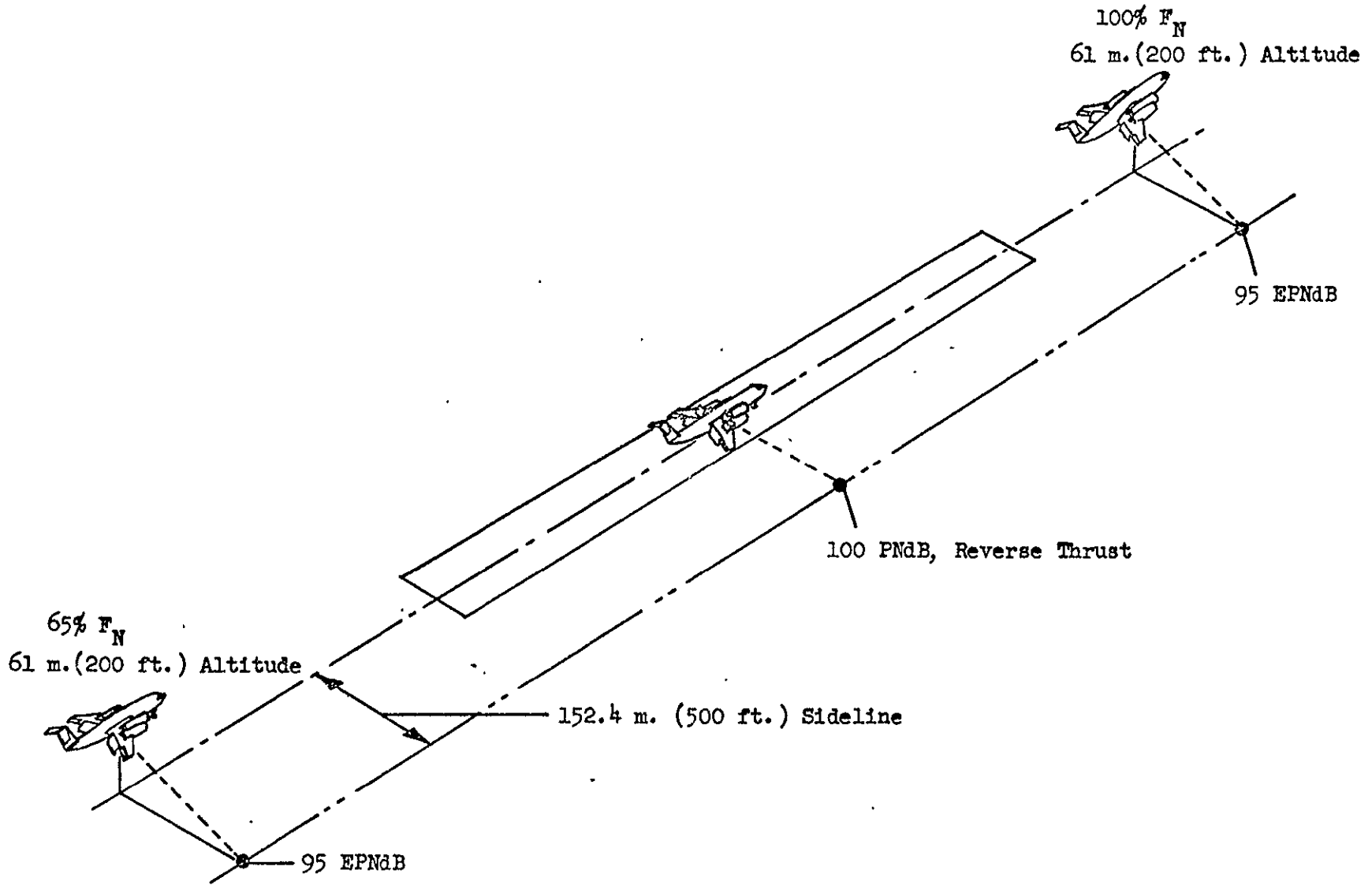


Figure 2 STOL Aircraft Noise Goals.

gross weight of 61,235 kg (135,000 lb) was chosen as being representative of first generation transports of this type. In order to meet 609.6 m (2000 ft) runway operational requirements, the wing area was sized for a moderate wing loading of 390.5 kg/m^2 (80 lb/ft^2), with takeoff and landing speeds of about 41 m/sec (80 knots). A cruise Mach number of 0.7 was assumed, and on this basis an unswept, tapered wing was selected. A partial plan view of the aircraft, showing the general wing configuration and engine installation is given on Figure 3. The wing planform has a taper ratio of 0.3 with a quarter chord sweep angle of 6.5° . Over all wing span is 36.5 m (119.76 ft); wing area is 156.8 m^2 (1687.5 ft^2).

Nacelle placement was established at 21% and 44% of wing semi-span, based on study data for similar installations (Reference 1); the propulsive lift D nozzle exit plane was positioned at 20% of the local wing chord. Four-engine thrust to aircraft takeoff gross weight was assumed to be 0.6 which establishes thrust per engine at 90,296 newtons (20,300 lb).

3.3 ENGINE CYCLE SELECTION

Engine cycle selection for the conceptual commercial STOL transport is highly dependent upon noise goals established for these aircraft when operated from short runways. In order to meet the noise goals in forward thrust, two sources must be evaluated: 1) that from the propulsion system and 2) the noise created by interaction of the jet exhaust with the wing and flap system during powered lift. Previous studies by General Electric (References 2, 3, 4, and 5) have shown that these two sources must be balanced such that the total noise will meet the 95 EPNdB requirement. The most effective system is one in which the engine and jet/flap levels are approximately equal. Thus the engine cycle must be selected such that engine suppression levels are reasonable and attainable and jet/flap noise is acceptable.

There are many parameters which define the level for both engine and jet/ flap noise, however, the most important is the fan pressure ratio. This determines the fan exhaust velocity which, in turn, establishes the

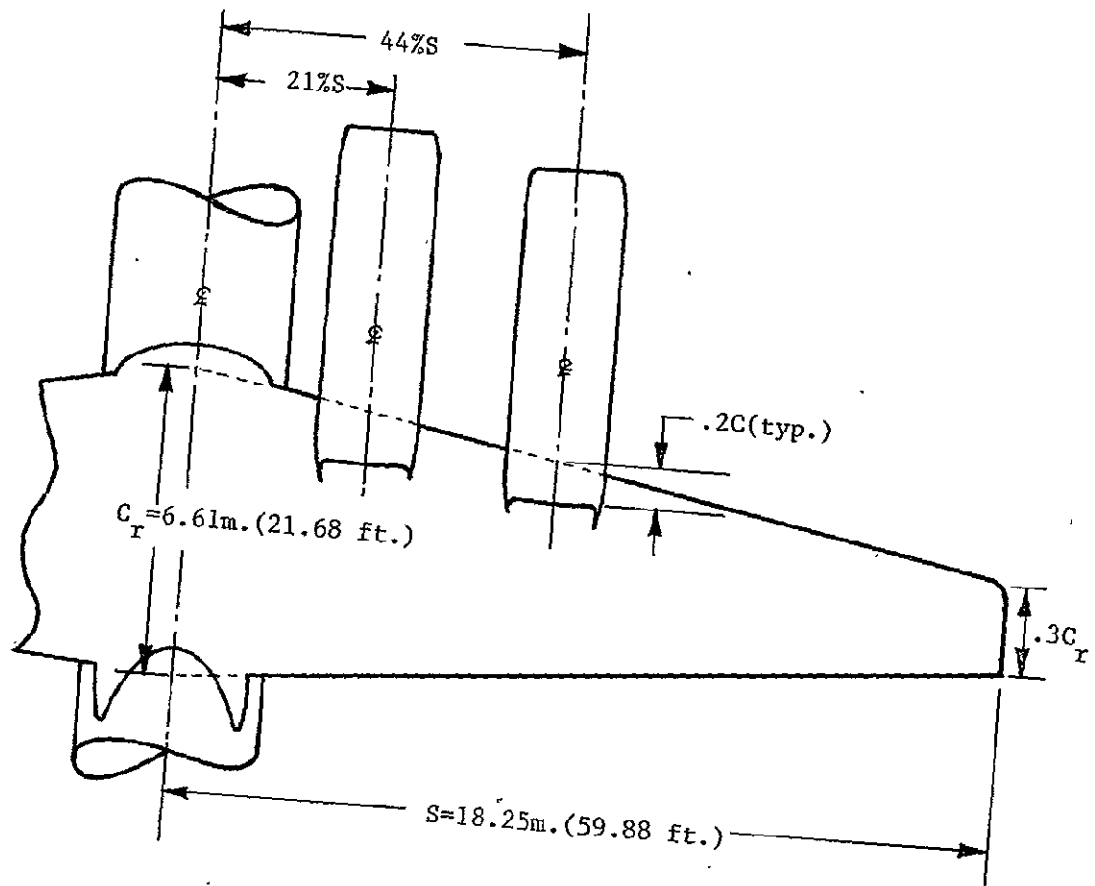


Figure 3 OTW STOL Transport Engine Installation.

jet/flap noise level. Generally this results in a 1.30 to 1.40 fan pressure ratio for an OTW system. At a fan pressure ratio of 1.3 to 1.40, the engine noise must be suppressed by approximately 10 PNdB to attain a balanced level equal to the jet/flap noise.

For this study, two mixed flow bypass ratio 10 turbofan cycles were chosen. The baseline cycle utilized a 1.34 pressure ratio fan; the second cycle employed a fan having a pressure ratio of 1.38. Figure 4 shows the takeoff constituent noise levels for an OTW commercial transport at the two cycle conditions. The jet/flap levels calculated for the study assumed an advanced technology noise reduction of 5 PNdB.

The higher pressure ratio cycle offers the potential for better engine cruise performance and lower drag at cruise (smaller nacelle diameter for required thrust). An additional advantage for thrust reversal is that for a given fan diameter, the higher pressure ratio cycle requires a smaller nozzle area. This condition provides an effectively larger upstream nacelle cross-sectional area (and volume) to facilitate installation of the thrust reverser for matching reverse mode cycle effective area.


The high bypass ratio (10:1) selected for these engine cycles provides high airflow rates required to meet takeoff gross thrust at low cycle pressure ratios. High flowing the engine at takeoff and landing approach conditions is achieved by opening the exhaust nozzle. At cruise, the nozzle closes to increase cycle pressure ratio for high propulsive efficiency. For the two cycles selected the area variation between takeoff and cruise nozzle settings is about 20%.

3.4 BASELINE NACELLE/NOZZLE CONFIGURATION

The nacelle and nozzle configuration required to satisfy commercial OTW STOL transport noise goals and exhaust flow field characteristics is shown schematically on Figure 5.

Attaining the low estimated noise levels required at takeoff and approach necessitates significant levels of engine suppression. This suppression must be attained in the fan inlet, fan exhaust, and core nozzle.

- 1.34 Fan Pressure Ratio Cycle
- 152.4m. (500 ft.) Sideline, 61m. (200 ft.) Altitude
- 4 Engines

 Suppression

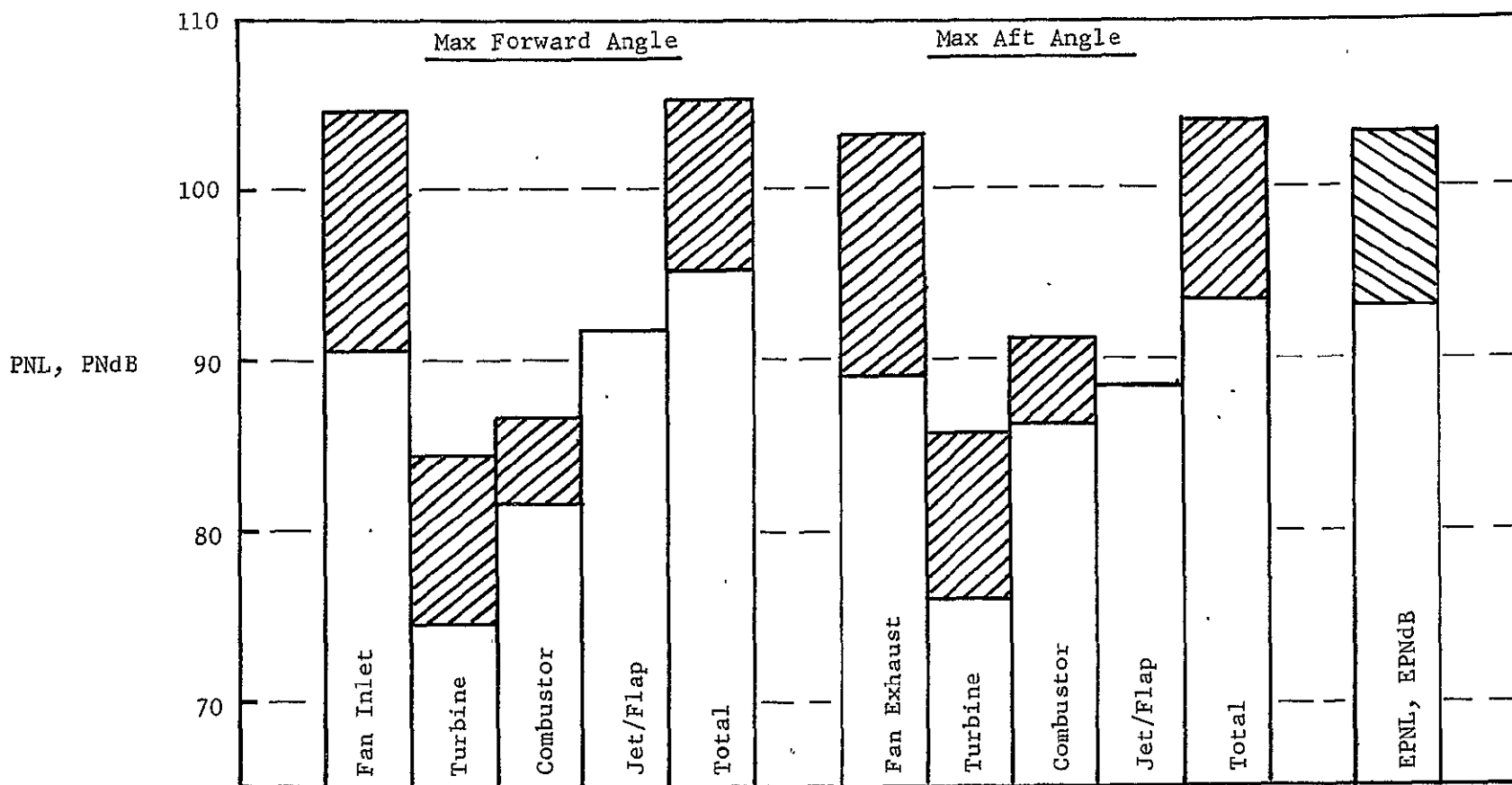



Figure 4a. Takeoff Noise Constituents.

- 1.38 Fan Pressure Ratio Cycle
- 152.4m. (500 ft.) Sideline, 61m. (200 ft.) Altitude
- 4 Engines

 Suppression

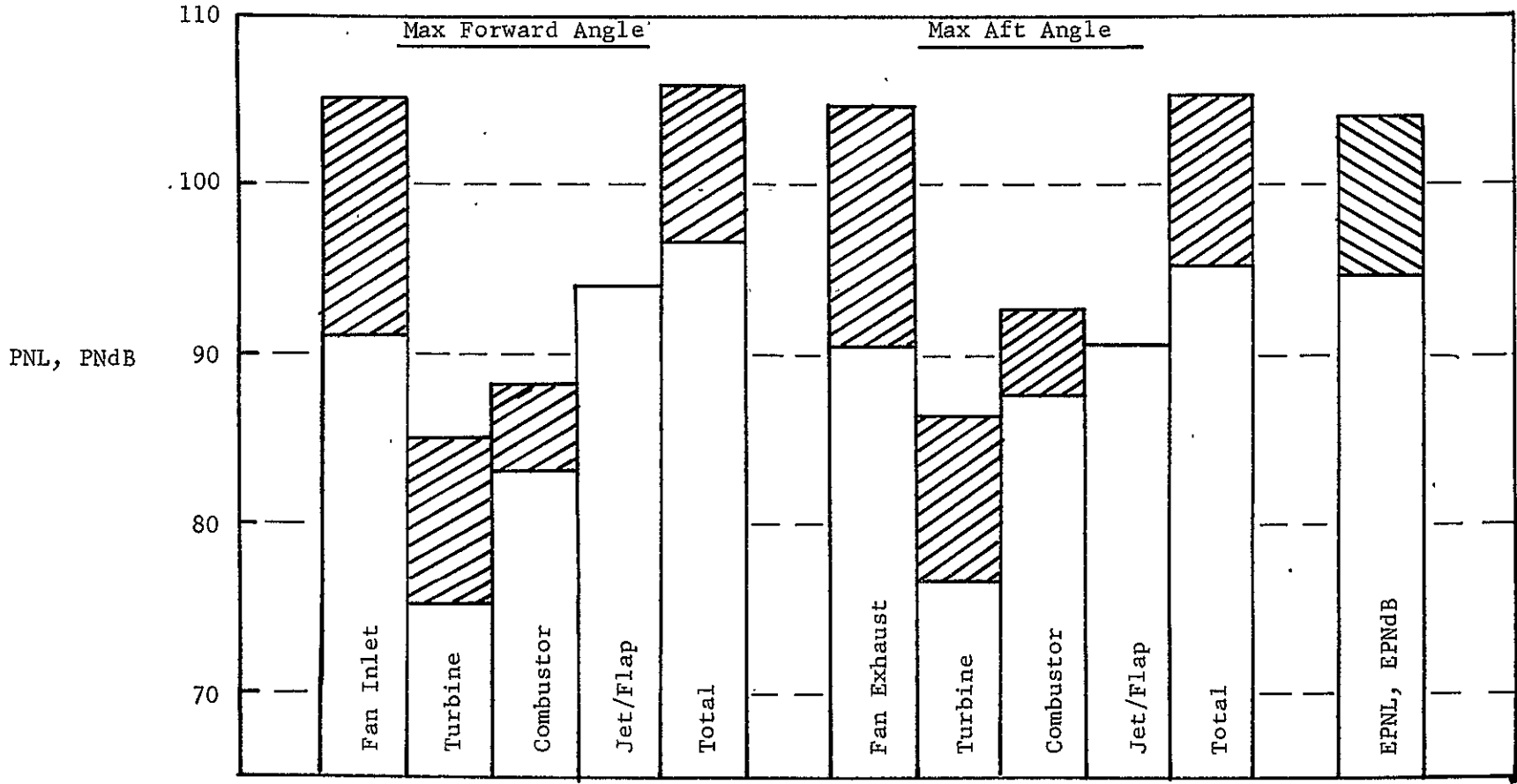


Figure 4b. Takeoff Noise Constituents.

$\frac{P_T}{P_0}$	D_{max}
1.34	2.0m. (6.56 ft.)
1.38	1.92m. (6.3 ft.)

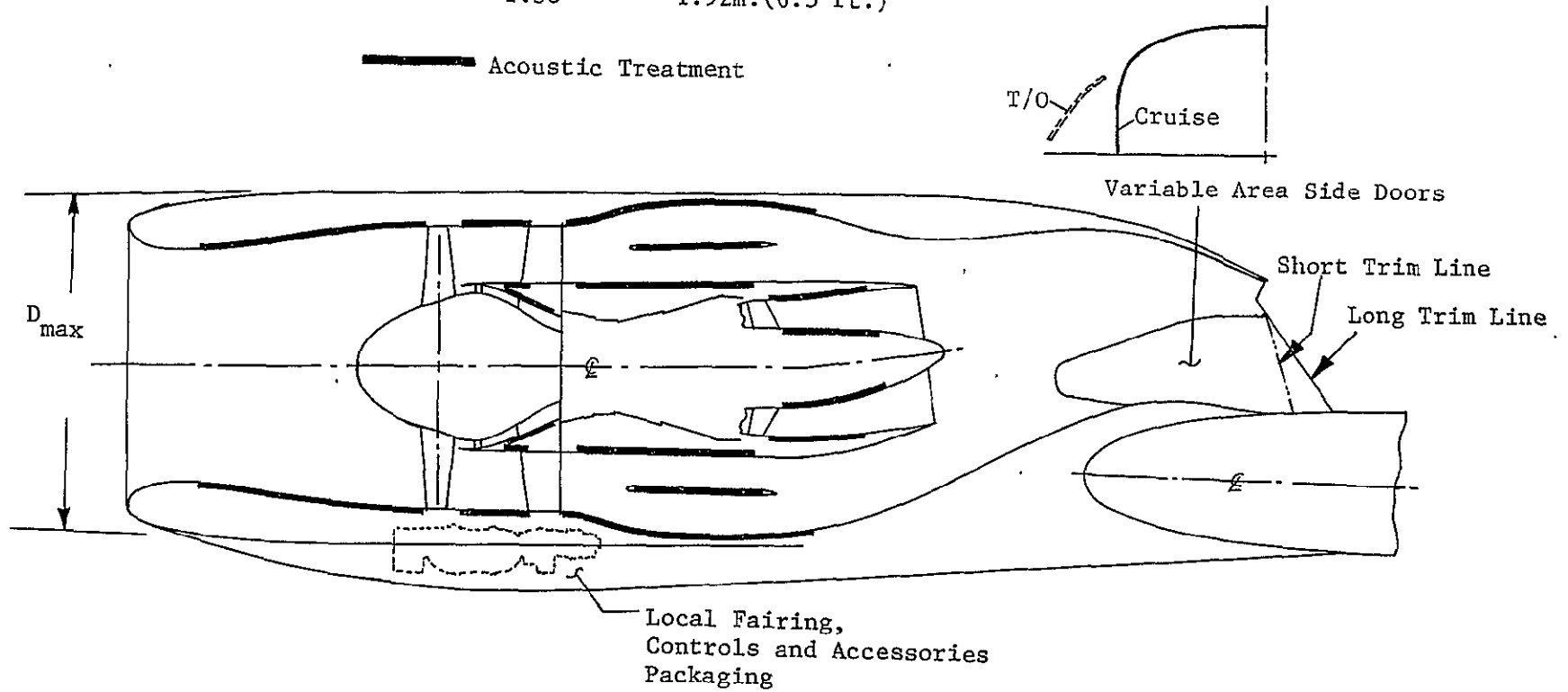


Figure 5 OTW STOL Transport Baseline Nacelle/Nozzle Configuration.

The nacelle design, as seen in Figure 5, is significantly influenced by the acoustic design requirements, particularly in the exhaust duct where the thrust reverser, variable area nozzle, and core nozzle must be integrated into an acceptable aerodynamic propulsion system configuration.

Acoustically, the fan exhaust duct must satisfy several requirements:

1. Treated outer and inner wall. The treatment must extend from the fan stator vanes aft a minimum of 0.9 fan diameter.
2. An acoustic splitter in the fan duct equal to 0.4 fan diameter.
3. Duct Mach number of 0.5 or less over the splitter region.
4. Nacelle outer-wall thickness sufficient to accept a minimum of 2.34 cm (1 inch) thick acoustic treatment.
5. Core nozzle length sufficient for outer and inner wall treatment equal to 0.7 turbine diameter.

Typical fan exhaust and core nozzle treatment configurations are shown in Figure 5. With this level of suppression both the cycle cases selected for the analytical study meet 95 EPNdB.

The fan inlet also was assumed to be suppressed by increasing the inlet throat Mach number. This does not affect the mechanical integration of the reverser into the nozzle but it is significant when operating the reverser. If the reverser design is such that it is operated at part power, or if it restricts the amount of air flow, then the high throat Mach numbers are not attained and only suppression from wall treatment is available.

The nacelle design makes use of thin wall composite technology for light weight and minimum nacelle diameter. The core nozzle is canted upward to minimize wing upper surface heat-up. The D nozzle provides cycle area variation side doors (closed for cruise, open for takeoff and landing) and spreads the exhaust flow for high propulsive lift performance as shown on Figure 5. The nozzle exit plane is trimmed long on one side and short on the other to help control low speed flow spreading onto the fuselage on inboard engines, and for limiting outward spreading beyond the propulsive lift flap system. Asymmetrically opening the two side doors may also be

used to provide additional flow spreading control. Nacelle maximum diameter for the 1.34 fan pressure baseline engine is 2.00 m (78.8 inches). For the 1.38 fan pressure derivative cycle the maximum nacelle diameter is 1.92 m (75.6 inches).

3.5 LANDING DISTANCE STUDIES

Aircraft landing distance analytical studies were made to explore the effects of engine power setting and reverser cut-off velocity (throttle retard to flight idle) on overall stopping distance. These studies were made for various ground roll conditions including icy, wet and dry runways and failed brakes. Study results are shown on Figure 6. These data show that thrust reversal at engine power settings as low as 40% (20% reverse thrust at a reverser effectivity of 50%) is sufficient to stop the STOL transport within the 609.6 m (2000 ft) requirement with reverser cut off velocities in the 5 to 10 m/sec (10 to 20 knots) range. These results show that throttled back engine operation during landing can be employed along with a high performance reverser to aid in achievement of reverse thrust noise goals.

Ground roll distances in Figure 6 were calculated using an available CTOL aircraft stopping distance computer program (Reference 6) modified to accommodate the assumed STOL transport engine cycle characteristics, aircraft aerodynamic configuration, and upward discharging reverser efflux effects on braking force. Data presented on Figure 6 include a 152.4 m (500 ft) air run distance (from a 10.7 m (35 ft) obstacle at end of runway to point of touchdown) in addition to the computed ground roll distance. Application of brakes and initiation of thrust reversal was assumed to have a one second delay time after touchdown. Throughout the ground roll aircraft lift and drag coefficients were held constant at $C_L = 1.0$ and $C_D = 0.15$ respectively. An upward discharging angle of 40° (β_e from Reference 7) was used to determine the reverser induced wheel loading component of total braking force.

Although not included on Figure 6, the effects of delay time and aircraft drag coefficient on landing distance were also investigated. A

- Gross Weight = 61235 kg. (135000 lbs.)
- Touchdown Velocity = 41 m/s (80 knots)
- Delay Time = 1.0 second
- Thrust/Weight = 0.6
- $S_w = 156.8 \text{ m}^2$ (1687.5 ft^2)
- Air Run Over End of Runway to Touchdown = 152.4 m. (500 ft.)

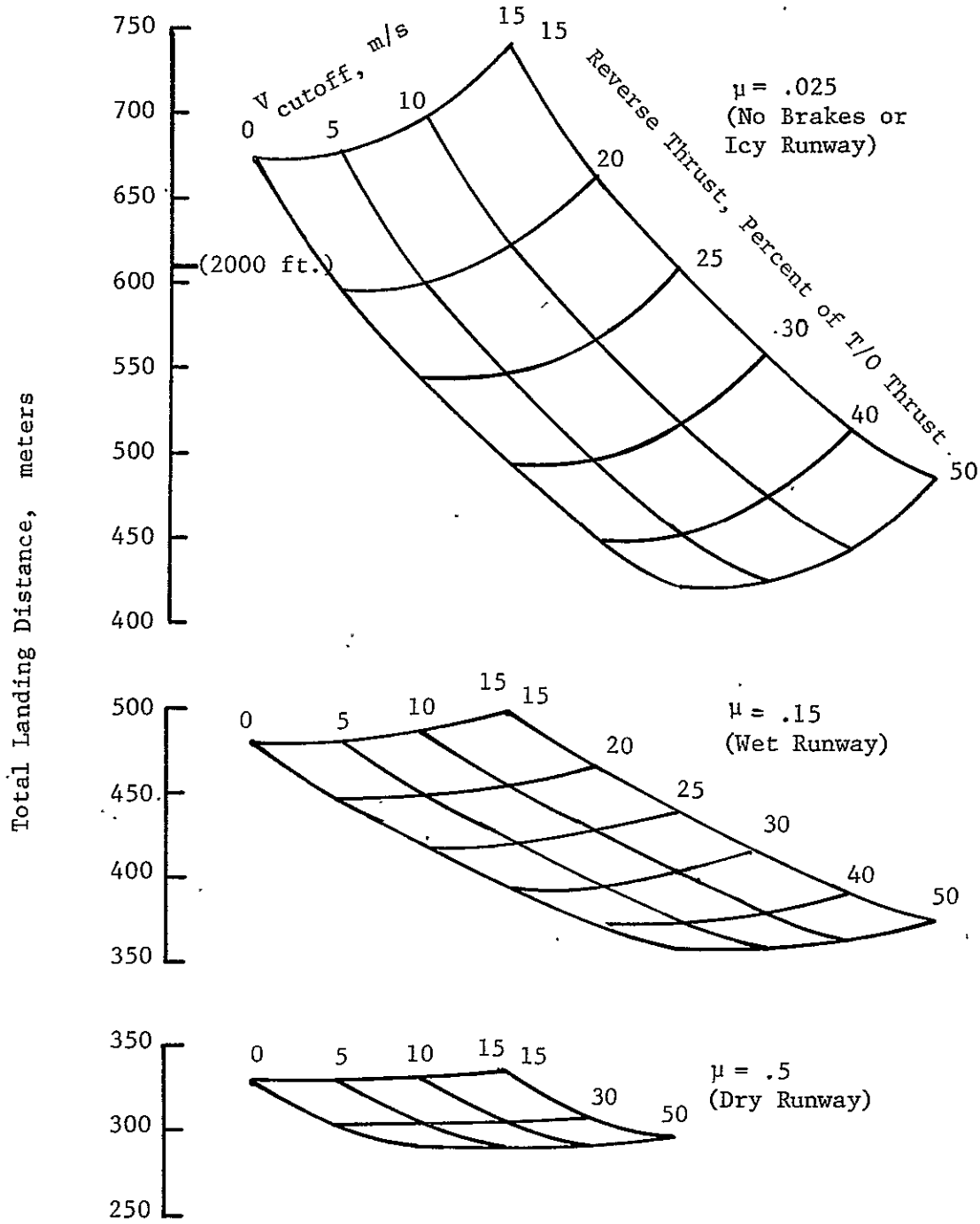


Figure 6 Landing Distance Parametric Study.

change in delay time of one-second (\pm) was shown to effect a 45.7 m (150 ft) change (\pm) in landing distance (independent of runway condition and power setting during reversal); on the other hand doubling the aircraft drag coefficient from 0.15 to 0.3 reduced landing distance from essentially 0 at high engine power and dry runways to about 45.7 m (150 ft) at low engine power (15%) reverse thrust, icy runway conditions. Upon applying these derivative effects to the data on Figure 5 it appears that some latitude in increased delay time is permissible except, perhaps, for icy runway or failed brake cases, where maximum runway rolls would exceed 609.6 m (2000 ft) at the low engine power levels. Under these most adverse emergency conditions it must be assumed that strict adherence to the normal operational noise restrictions is waived for passenger and equipment safety, and engine power increased as required for stopping.

3.6 THRUST REVERSER CONCEPTUAL DESIGN

Thrust reverser design studies were conducted to establish aerodynamic flowpaths, estimated aerodynamic and acoustics performance characteristics of three OTW nacelle reverser concepts which meet the objective of 50% reversal:

- Integral D nozzle/single blocker target reverser
- Integral D nozzle/top arc cascade reverser
- Post exit target reverser integral with wing upper surface.

Mechanical layouts were made of each concept to establish an integrated reverser/nacelle arrangement having good internal and external aerodynamic lines. Reverser actuation systems and kinematic linkages were studied in sufficient detail to assure that a viable concept evolved for each configuration. General Electric folder series drawing which define these configurations respectively are as follows:

Drawing 4013237-436 (single blocker target)
4013237-443 (top arc cascade)
4013237-439 (port exit target)

3.6.1 Integral D Nozzle/Single Blocker Target Reverser

The single blocker target reverser contained within the nacelle appeared to be one of the more attractive thrust reversal concepts available for OTW STOL transport application. Its integration into the nacelle takes advantage of maximum hardware commonality for light propulsion system weight. Its upward discharging efflux virtually eliminates reingestion and thereby provides the very low ground speed utilization required for these aircraft. The conceptual reverser design which evolved from this study is shown on Figure 7. It is a single blocker door design with the door forming the top section of the D shaped nozzle in the forward thrust position. The blocker door trim lines were positioned so as not to interfere with normal operation of the nozzle variable area side doors. The blocker door pivot and forward trim line were selected to provide the required axial spacing and blocker door projected area. Final reverse flow direction is given to the engine exhaust by means of a blocker lip which stows on the external (back) side of the main blocker and articulates forward to a 25° position during reversal. Variable position side skirts attached to the main blocker are also employed to provide additional blocker capture area for minimum side spillage. In reverse, these skirts rotate outward 45°; when the reverser is stowed the skirts nest in recesses provided in the nacelle structural side walls.

Reverser actuation is accomplished by means of a single actuator mounted on the top of the nacelle. The blocker lip is articulated automatically by the main blocker rotation through a link arrangement attached at one end to the blocker lip and at the other end to the structural side wall near the blocker pivot. The side skirts are similarly operated through a linkage system between the blocker lip and the skirts.

The aerodynamic flowpath and estimated reverse thrust performance of this conceptual design was derived from the data base obtained from tests on a similar configuration (including side skirt geometry) as reported in Reference 7. Reverse thrust performance from these referenced tests showed a reverser effectiveness of 38 to 40% (F_{rev}/F_{fwd} at the same pressure ratio) with a coincident 20% reduction in reverse mode airflow capacity

Geometric Parameters

$$\beta = 25^\circ$$

$$H/D_{th} = 1.73$$

$$L/D_{th} = 0.4$$

$$X/D_{th} = 1.1$$

$$A_{290}/A_{T/O} = 1.62$$

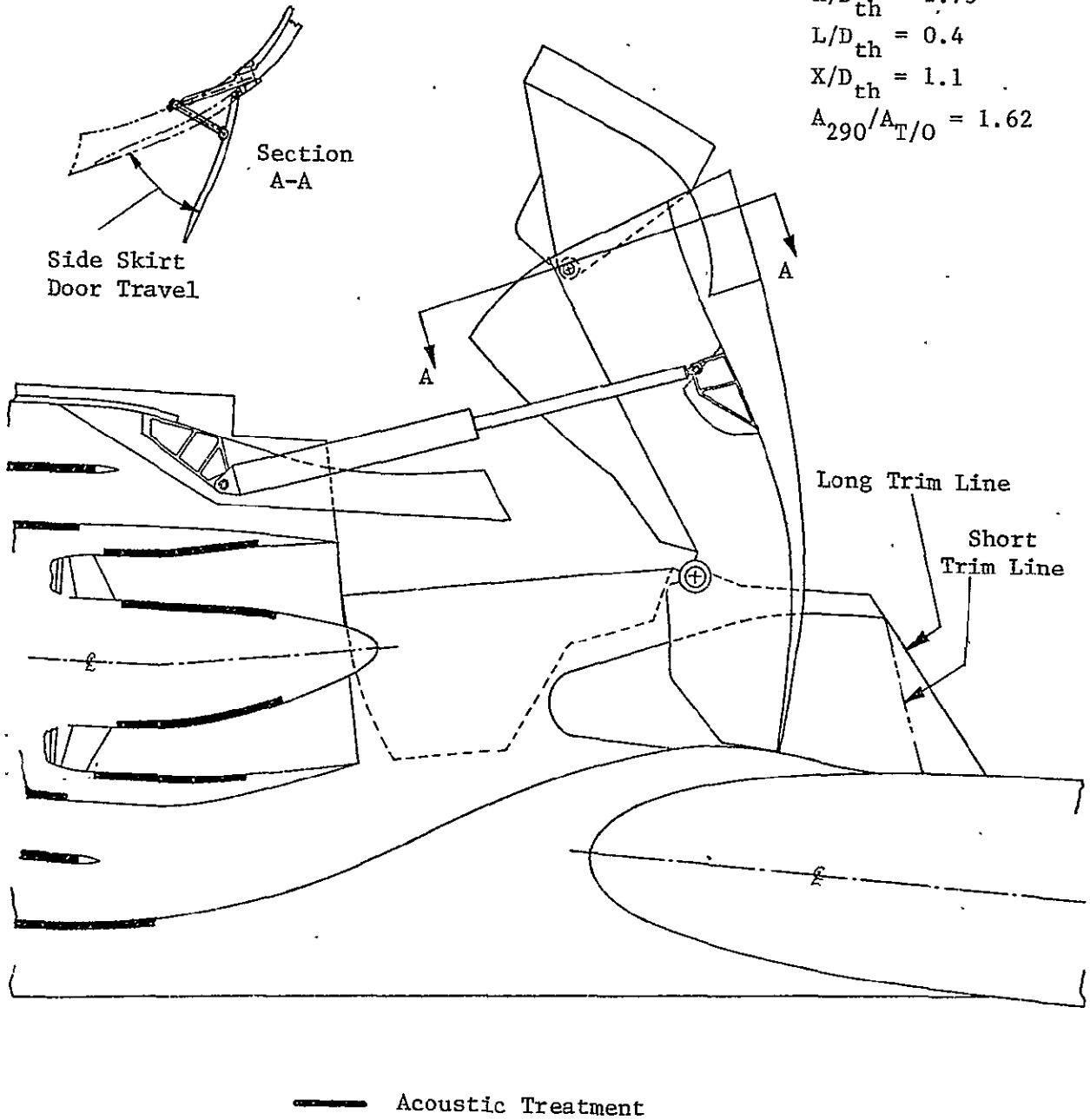


Figure 7 Integral D Nozzle and Target Reverser.

(cycle area mismatch) relative to the forward mode takeoff thrust conditions. In order to establish a conceptual design having 50% thrust reversal without reduction in airflow capacity, changes were made to both the reference reverser configuration and nacelle internal flowpath. Table 1 compares the resultant conceptual design geometry with the data base values. As shown, the blocker door height was increased slightly and the charging station (Station 290) width to height ratio (W/D_{th}) and area ratio ($A_{290}/A_{T/O}$) were significantly increased. These last two changes provided the greatest benefit to the conceptual reverser performance: The charging station area increase provides additional flow capacity in reverse to overcome the cycle area mismatch found to occur on the Reference 7 configuration, and also produces a corresponding increase in reverser effectiveness amounting to 10 points. Increasing the aspect ratio from 1.063 to 1.245 effectively widens the blocker for better containment of the reversed flow and provides an estimated additional improvement of about 2.5 points. The combined effects bring the estimated performance of the conceptual target reverser design up to the 50% objective level. Figure 8 shows the estimated results, along with the data base extracted from Reference 7.

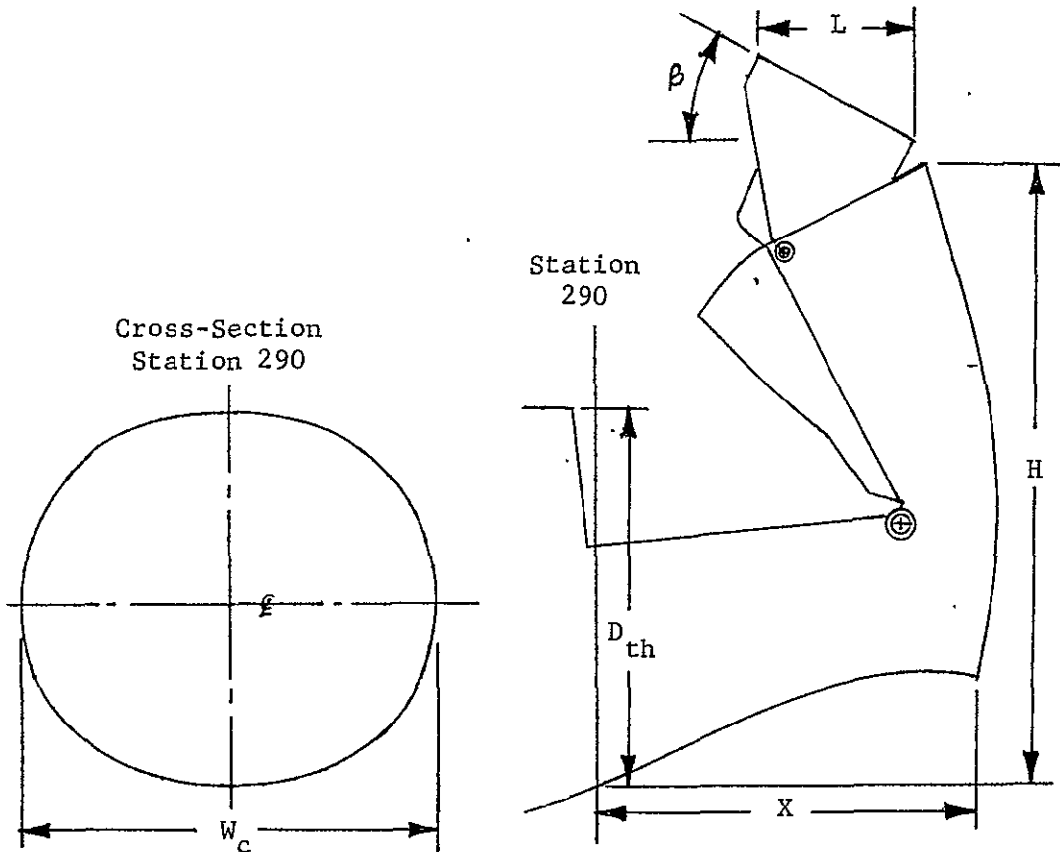
Achievement of the objective reverser estimated performance was not without compromise to nacelle design. The increase in charging station area (Station 290) required to eliminate cycle area mismatch forced nacelle diameter to increase nearly 12% (from 2.0 meters to 2.233 meters for the 1.34 fan pressure ratio cycle and from 1.92 meters to 2.144 meters for the 1.38 fan pressure ratio cycle). On an isolated nacelle basis, the increased diameter required for integration of the high performance single blocker target reverser concept penalized cruise nacelle drag by an estimated 2-3% of cruise net thrust. Installation of the reverser concept was not found to affect forward thrust nozzle performance, nor did it affect the extent of acoustically treated surfaces required within the fan and core nozzle ducting.

Noise estimates were made for each cycle with both the baseline charging station area and an increased charging station area. Although the baseline duct was shown to backpressure the fan (Reference 7) which is not

Table I
 Comparison of Conceptual Target Reverser Geometric
 Parameters with Reference Configuration

<u>Reverser Parameter</u>	<u>OTW STOL Transport Reverser Conceptual Design</u>	<u>Reference 7 Data Base Configuration</u>
β	25°	25°
H/D_{th}	1.73	1.63
L/D_{th}	0.40	0.40
X/D_{th}	1.10	1.11
$(W_c/D_{th})_{290}$	1.245	1.063
$A_{290}/A_{T/O}$	$\left\{ \begin{array}{l} 1.62 \text{ (1.38*)} \\ 1.52 \text{ (1.34*)} \end{array} \right.$	1.146 (1.34*)

* Indicates cycle fan pressure ratio

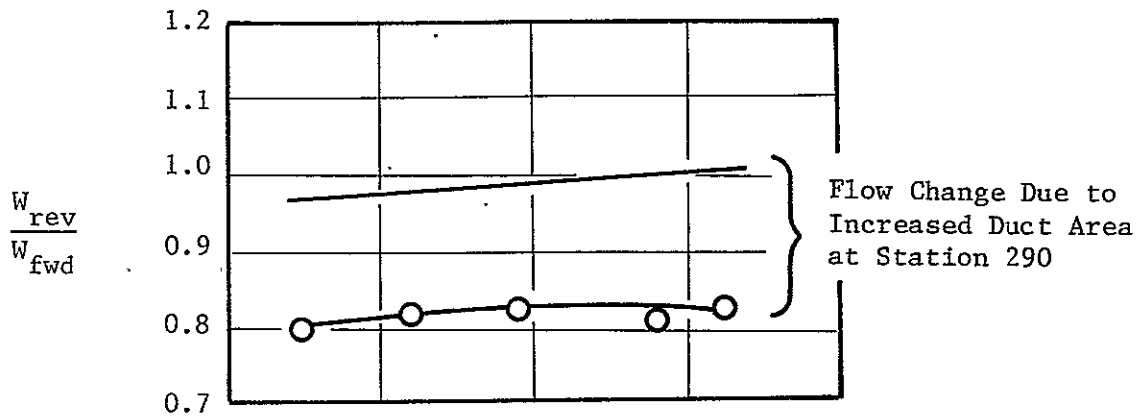


Geometric Parameters

$$\beta = 25^\circ \quad H/D_{th} = 1.73$$

$$L/D_{th} = 0.4 \quad X/D_{th} = 1.1$$

$$A_{290}/A_{T/O} = 1.62$$



————— Estimated Reverser Performance NASA Ames Study
 ○—○—○ NASA Langley Scale Model Data (Reference 7)

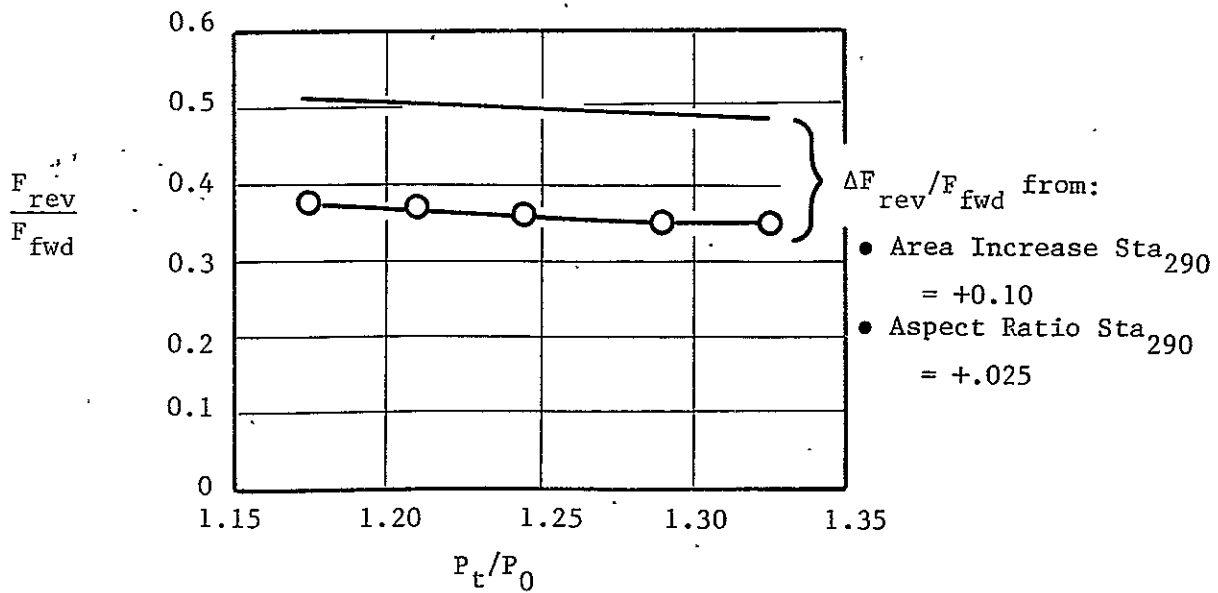


Figure 8 Target Reverser Performance

acceptable for the study ground rules, noise calculations are presented to demonstrate the benefit of fan duct design on reverse thrust noise.

Analysis of each duct and cycle combination was accomplished using the data presented in Reference 8. From this data the noise levels were estimated with the primary variation occurring with changes in the velocity at the charging station. Spectral analysis was also found to be dependent upon this velocity over the range of velocities associated with the designs. The noise estimates were calculated for a 152.4 m (500 ft) sideline at forward thrust power settings from 40% to 100%. Results are shown on Figure 9 for both of the duct geometries and the two cycle conditions. For the baseline duct case, the cycle variation is not evident because of the backpressure created by the reverser. The effect of reducing the velocities at the charging station is seen dramatically by comparing the estimates for the large and small ducts. The large duct configuration is 6 to 11 PNdB quieter than the baseline duct high velocity configuration.

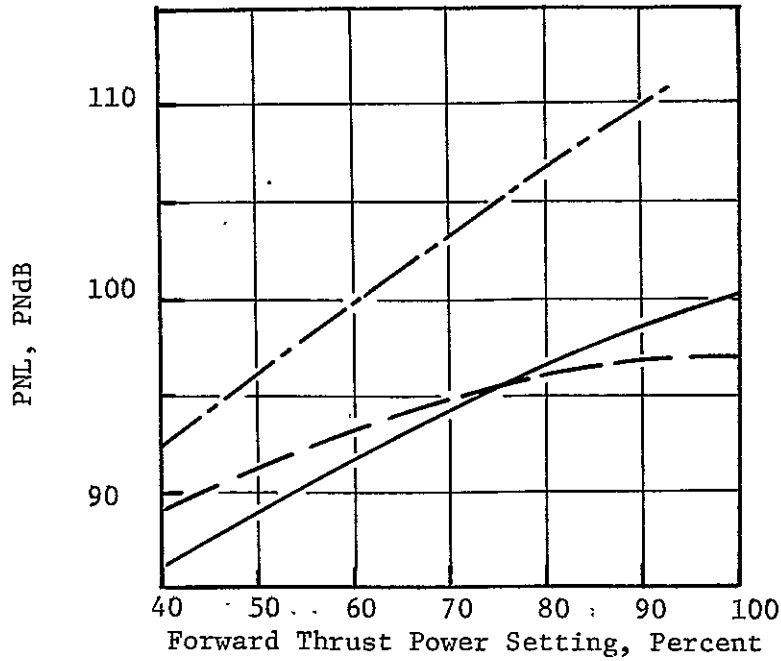
These thrust reverser estimated noise levels were combined with estimated engine noise to obtain total noise on a 152.4 m (500 ft) sideline. Other sources included fan inlet, fan exhaust, core and turbine noise. Aft radiated noise was assumed to be directed along the same axis as the efflux of the reverser gas thus the maximum noise on the sideline occurs in the forward quadrant. Figure 10 shows the engine constituents at 50% power setting. The engine source noise PNdB levels are also shown on Figure 9. Both thrust reverser and engine noise were combined to provide total system noise for a 4 engine 61,235 kg (135,000 lb) gross weight aircraft. Figure 11 shows total estimated noise as a function of reverse thrust divided by takeoff thrust. In order to meet a maximum total system noise of 100 PNdB, the reverser must be operated at or below 40.5 to 43% reverse thrust with the open duct and 22.5% with the baseline duct. Engine stopping distance studies, Section 3.5, have shown that both of these reverse thrust levels are adequate to stop the aircraft.

Spectrally, the target reverser is low frequency in nature with a peak in the region of 160 Hz for the study size. The spectra varies with velocity but over the range of power settings evaluated the variation is

• 152.4 m. (500 ft.) Sideline

• 4 Engines

• 1.34 Fan Pressure Ratio Cycle



— Open Duct
 - - - Baseline Duct
 - · - Engine Noise

} Thrust Reverser Noise

Geometric Parameters

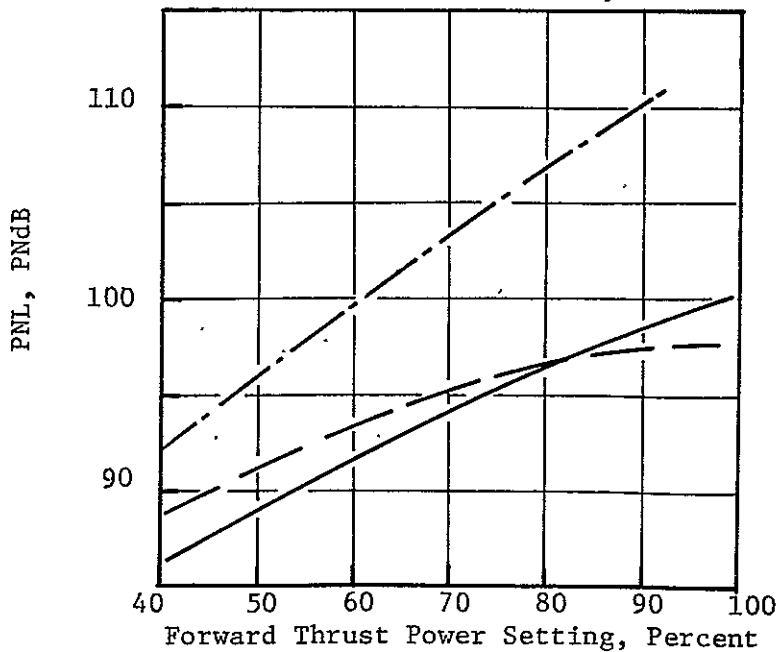
$$\beta = 25^\circ$$

$$H/D_{th} = 1.73$$

$$L/D_{th} = 0.4$$

$$X/D_{th} = 1.1$$

• 1.38 Fan Pressure Ratio Cycle



Fan Press. Ratio	1.34	1.38
$\frac{A_{290}}{A_{T/O}} = \begin{cases} \text{Baseline} \\ \text{Open} \end{cases}$	1.146	1.22
	1.52	1.62

Figure 9. Integral Target Reverser Noise.

- 152.4 m. (500 ft.) Sideline
- 4 Engines
- Suppressed
- 50% Forward Thrust Power Setting
- 1.34 Fan Pressure Ratio at Takeoff

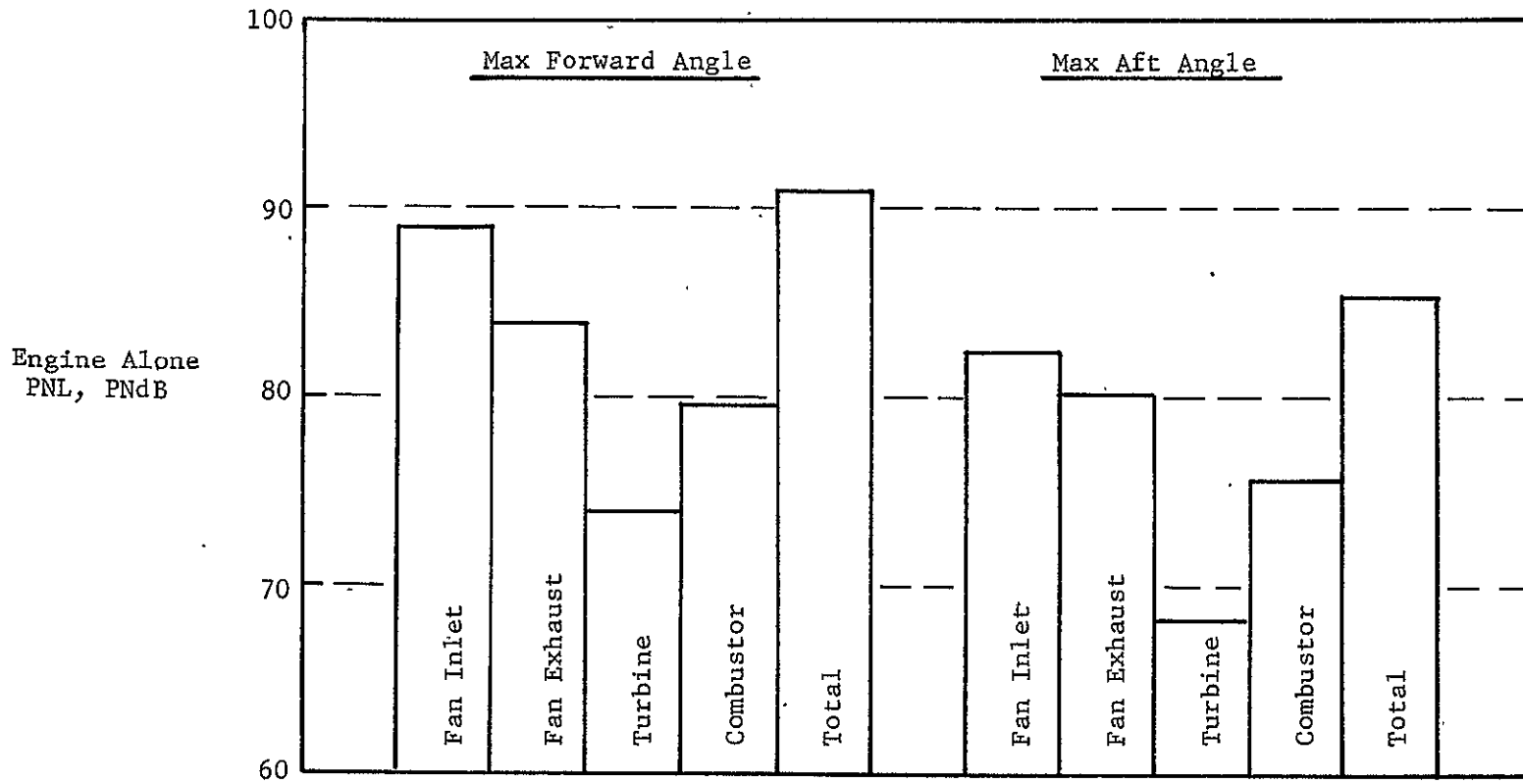


Figure 10 Engine Noise Constituents in Reverse Thrust.

Geometric Parameters

$$\beta = 25^\circ \quad H/D_{th} = 1.73$$

$$L/D_{th} = 0.4 \quad X/D_{th} = 1.1$$

Fan Pressure Ratio		1.34	1.38
$A_{290}/A_{T/O}$ for:	Open Duct	1.52	1.62
	Baseline Duct	1.146	1.22

- 152.4m. (500 ft.) Sideline
- 4 Engines

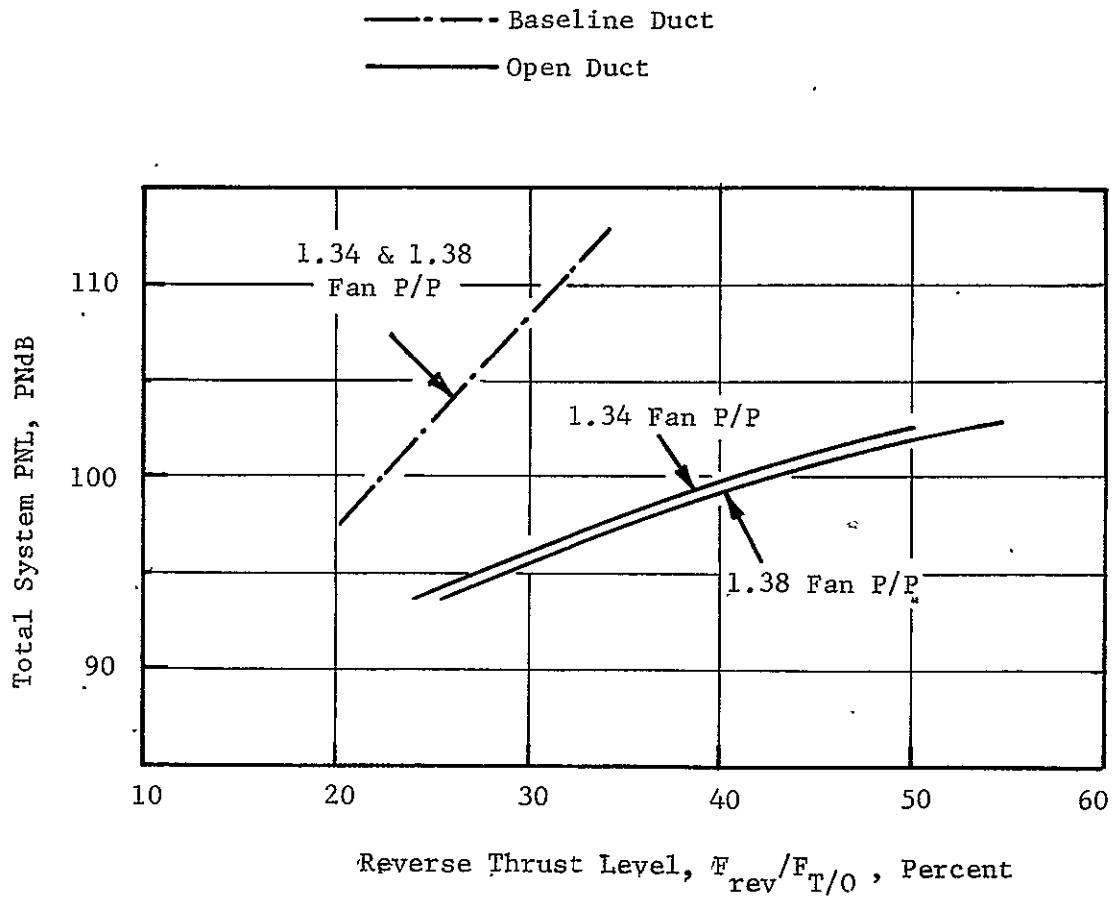


Figure 11 Total System Reverse Thrust Noise with Integral Target.

within one octave band. Figure 12 shows a typical target reverser spectra at 100 PNdB total system noise.

3.6.2 Integral D Nozzle/Top Arc Cascade Reverser Concept

Top arc cascade reversers have been considered previously (References 9 and 10) for potential use on STOL transports. In the references cited, these cascade reversers were assumed to be installed in annular fan ducts of high bypass ratio turbofan engines. The top arc discharge was obtained by blocking off the lower half of the cascade circumference. The cascade box axial length was increased to maintain the correct engine cycle area match, taking into consideration the additional total pressure losses which result from flow redistribution within the duct.

The concept also has potential for use on the OTW STOL transport. As with the integral target reverser concept discussed in Section 3.6.1, the top arc cascade concept shows promise for making extensive use of the exhaust ducting for light weight design. As shown on Figure 13, integration of this concept into a non-axisymmetric D shaped nozzle with variable area side doors required some unique aero/mechanical design approaches. The reverser cascade section, which consists of 14 boxes mounted around the top half of the nacelle, is positioned well aft in the mixed flow portion of the exhaust ducting. In flight the cascades are exposed to free stream flow, the thickened boundary layer on the nacelle aft section minimizing drag losses over the cascade vane trailing edges (possible industry trend, as indicated from Reference 11). In forward thrust position the cascades are sealed off internally by the common exhaust ducting. In reverse thrust position the inner ducting translates aft on three "tee" tracks to expose the cascades. Two links between the translating inner ducting and a blocker door which is normally stowed in the D nozzle floor, simultaneously lift the blocker door to seal the duct and redirect the exhaust gases into the cascades. The D nozzle cross sectional geometry in the region of the variable area side doors has been configured so that movement of the inner ducting and tee track assembly is without interference with the side doors in the fully closed (cruise and reverse) position. Reverser actuation is

- 152.4 m. (500 ft.) Sideline
- 4 Engines
- 40.5 Percent Thrust, $F_{rev}/F_{T/O}$
- 1.34 Fan Pressure Ratio Cycle, Open Duct

Geometric Parameters

$$\beta = 25^\circ \quad L/D_{th} = 0.4$$

$$H/D_{th} = 1.73 \quad X/D_{th} = 1.1$$

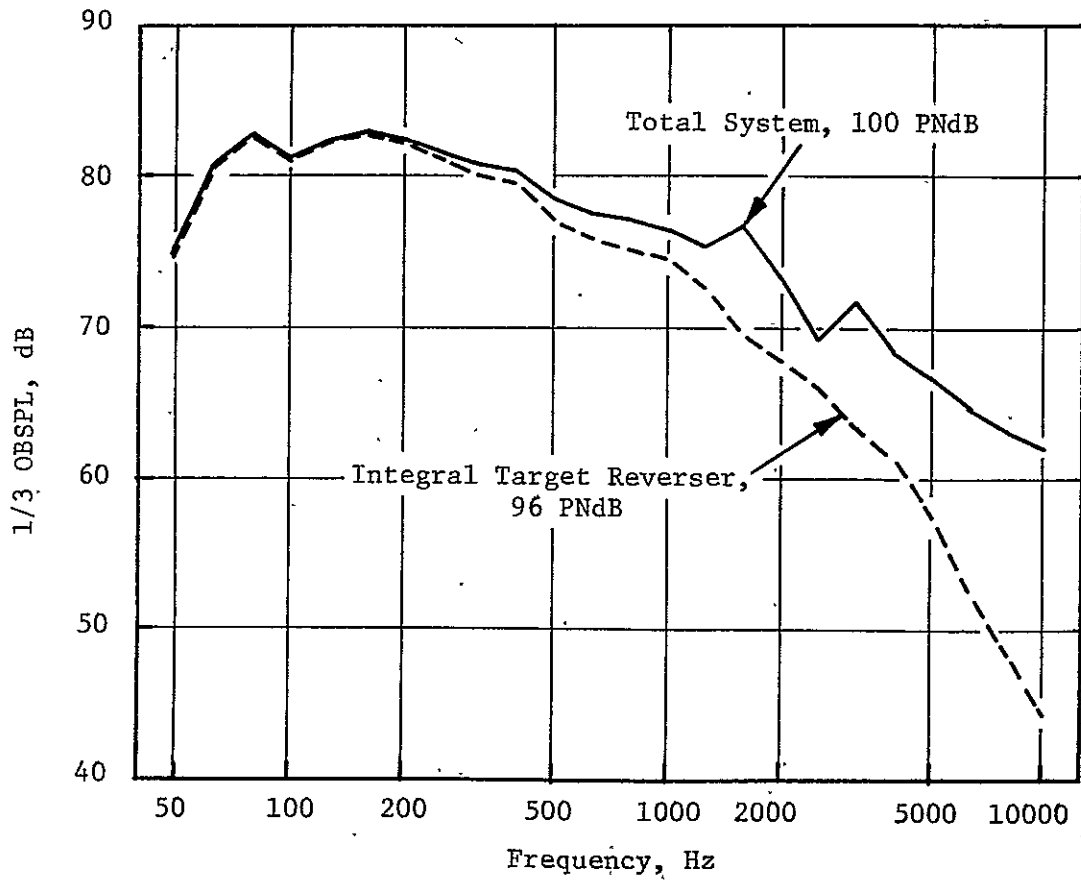


Figure 12. Integral Target Reverse Thrust Spectra

Geometric Parameters

$$\beta = 45^\circ \quad L_c = 1.245 \text{ m.}$$

$$P = 2.884 \text{ m.} \quad \alpha = 35^\circ$$

$$A_{290}/A_{T/O} = 1.22$$

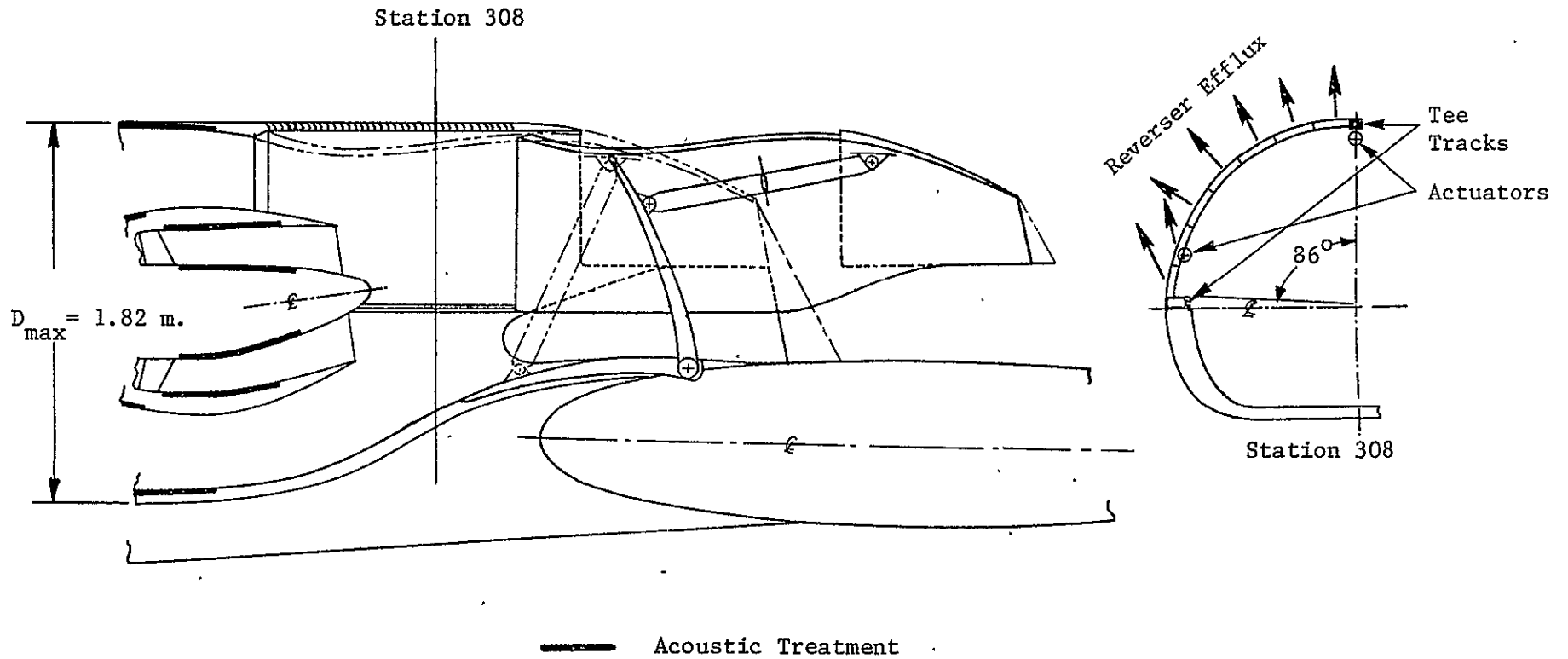


Figure 13 Integral D Nozzle and Top Arc Cascade Reverser.

accomplished by three actuators positioned around the portion of circumference used for the cascade section.

Reverser parametric design studies were conducted to establish the cascade length and circumferential extent required for cycle area matching and also to establish the discharge angle to meet the objective 50% reversal. In these studies internal ducting total pressure losses and cascade flow coefficient level were estimated from Reference 9. Cascade area allowance was made for actuator, tee track and cascade box structural blockages. An additional cascade area allowance was made to provide for on-wing efflux tailoring (upward skewing of flow and selectively blocking off cascade segments for best reverser installation performance). The results of these parametric design studies are given on Figures 14 and 15. All points on the sizing matrix, Figure 14, satisfy cycle area matching requirements as just discussed. The matrix shown on this figure was established for the 1.38 fan pressure ratio cycle. A similar sizing matrix for the lower fan pressure ratio (1.34) cycle would show a slightly longer cascade length required to match the larger cycle area at a given circumferential extent. The point within the sizing matrix which is selected ultimately is dependent upon the reverser cascade discharge angle required to meet the 50% thrust reversal objective with an assumed efflux skew pattern. For the configuration shown on Figure 13, a skew angle of 35° was chosen. It was assumed further, that on-wing tailoring might require up to about 30 percent (four out of 14) of the cascades to be skewed. The skew angle and efflux pattern selection was based on current CTOL reverser experience which indicates satisfactory efflux tailoring capability with moderate percentages (up to 40%) of cascade boxes skewed at this angle. As indicated from Figure 15, a cascade discharge angle of 46° or lower would be required to obtain the estimated objective performance with 30% of the cascades skewed 35° . A 45° discharge angle was selected for this conceptual design. From Figure 14, cascade length and circumferential wrap dimensions were matched at 1.245 m (49.96 in.) and 2.884 m (113.55 in.) respectively for the 45° efflux angle.

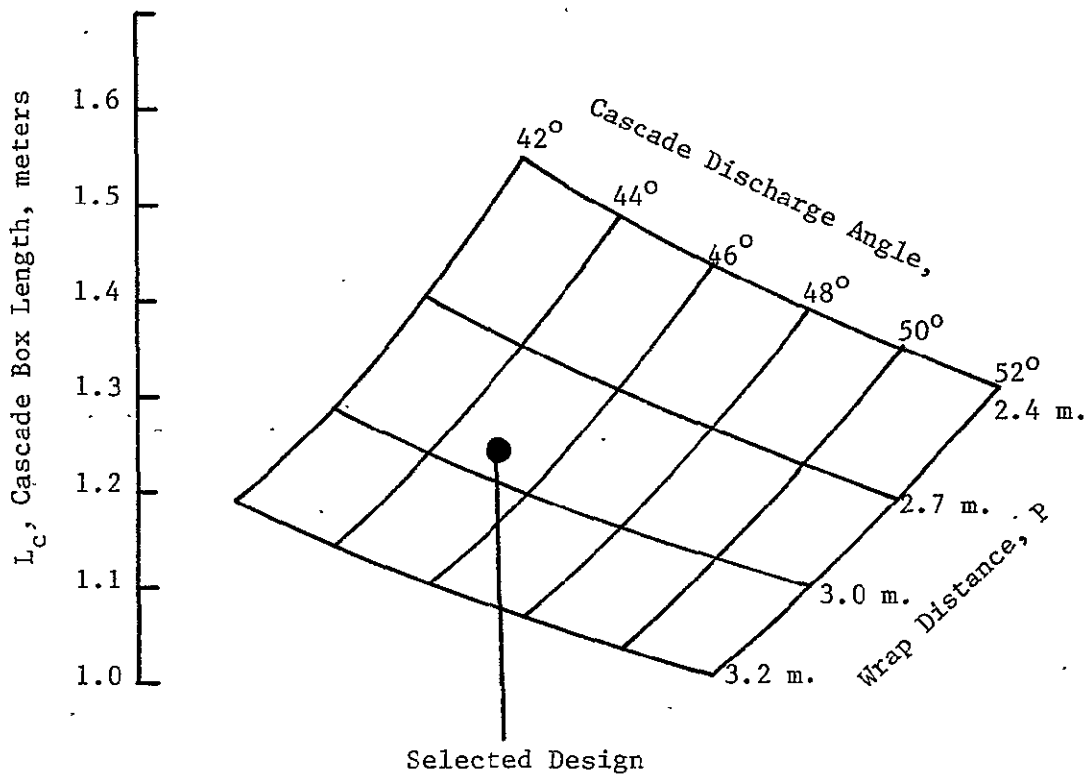
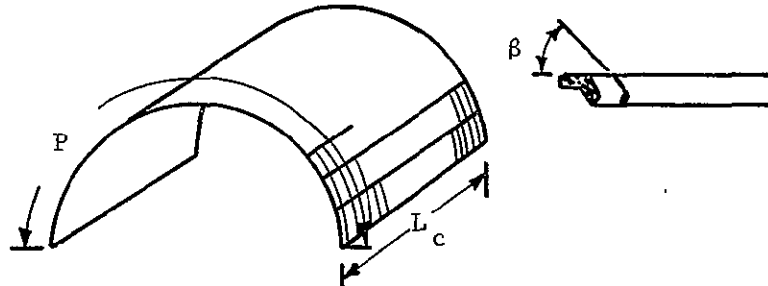


Figure 14 Top Arc Cascade Reverser Area Sizing Study.

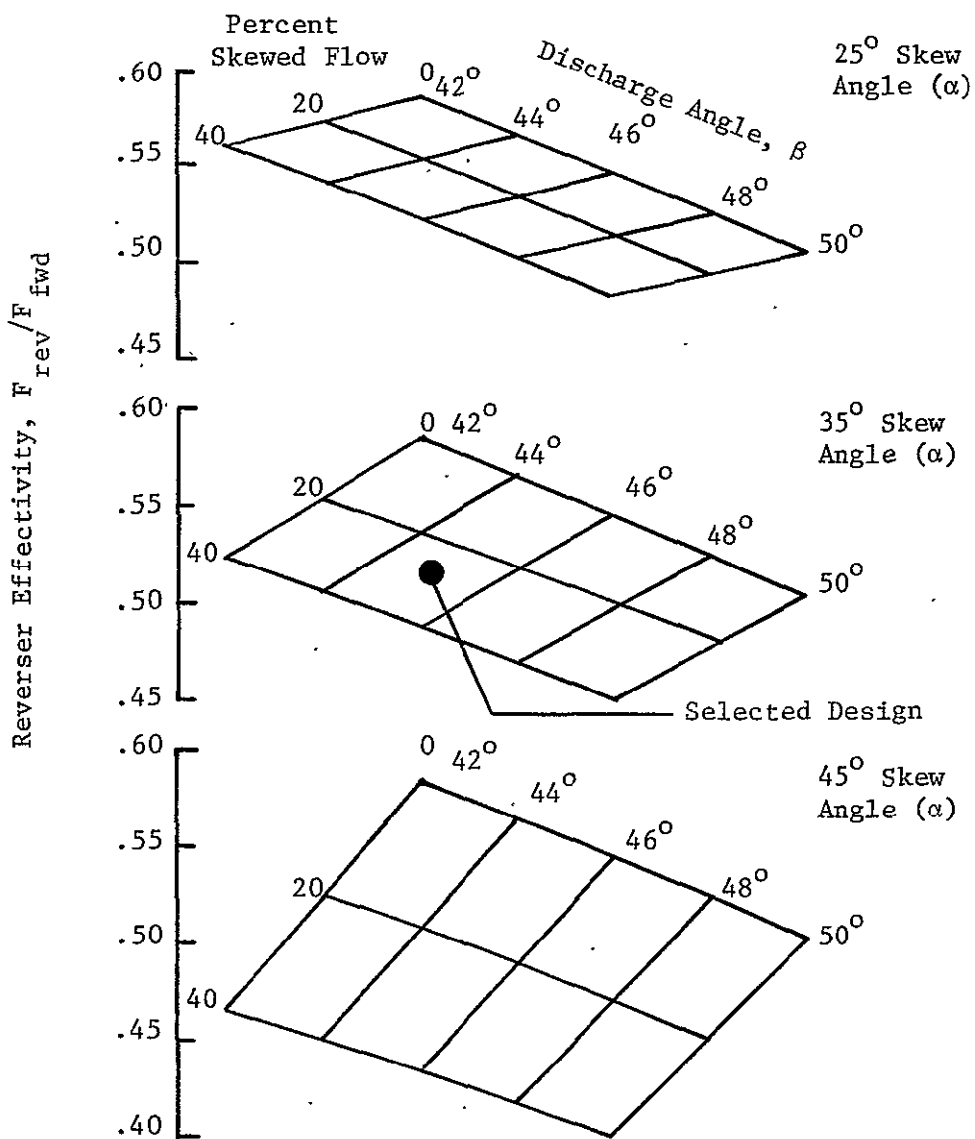
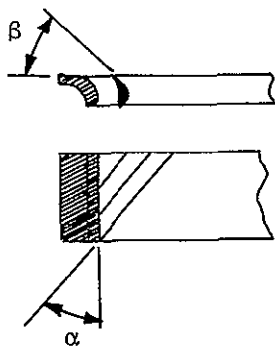


Figure 15 Top Arc Cascade Thrust Reverser Parametric Performance.

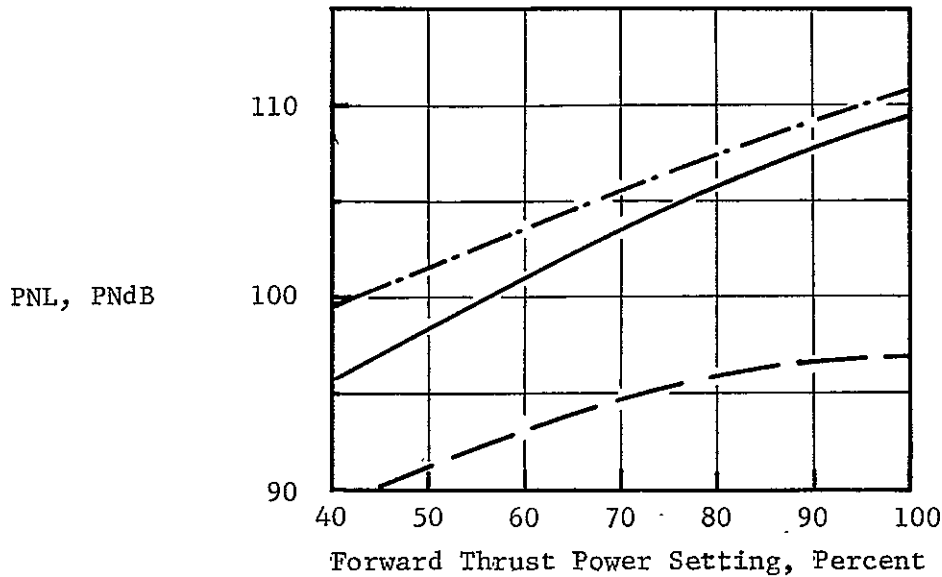
Top arc cascade reverser design studies have shown that this concept can be installed within the OTW D nozzle without compromising either cruise drag as a result of increased nacelle maximum diameter, or the D nozzle exit geometric requirements for good propulsive lift performance.

Cascade reverser noise estimates were made using the data of Reference 12 for both cycles with the baseline duct and with a larger diameter nacelle having lower duct Mach numbers. Although the larger duct is not required with the cascade, the data are presented for comparison. Analysis of the data provided a correlation of noise with the velocity entering the cascade and the velocity at the cascade exit. Each velocity contributed to the total noise with the velocity entering the cascade having the heaviest weighting. As with the target configurations, the larger fan exhaust duct with lower velocity entering the cascade has lower noise levels. This is shown in Figure 16. As the fan pressure ratio increases due to a cycle change the cascade velocity does not vary to a large degree because there is a trade between lower flow and increased pressure ratio which holds velocity almost constant. Other engine sources, as discussed in Section 3.6.1 are also shown on Figure 15. The total system noise for a 61,235 kg (135,000 lb) aircraft as a function of reverse thrust divided by takeoff thrust is shown in Figure 17. With the baseline duct and 1.38 fan pressure ratio cycle a thrust level of 20% will meet the 100 PNdB goal and is adequate for stopping the aircraft.

A typical cascade spectra is shown in Figure 18 for the baseline duct at 20% reverse thrust. The peak level occurs at approximately 800 Hz which is much higher than the peak target reverser levels. This higher frequency noise has the advantage of being more easily controlled within the aircraft cabin but has the disadvantage of higher farfield PNdB levels for the same overall sound pressure level. At a distance of 152.4 m (500 ft) the advantage of atmosphere attenuation is negligible.

- 152.4m. (500 ft.) Sideline
- 4 Engines

• 1.34 Fan Pressure Ratio Cycle



Geometric Parameters

$$L_c = 1.295 \text{ m.}$$

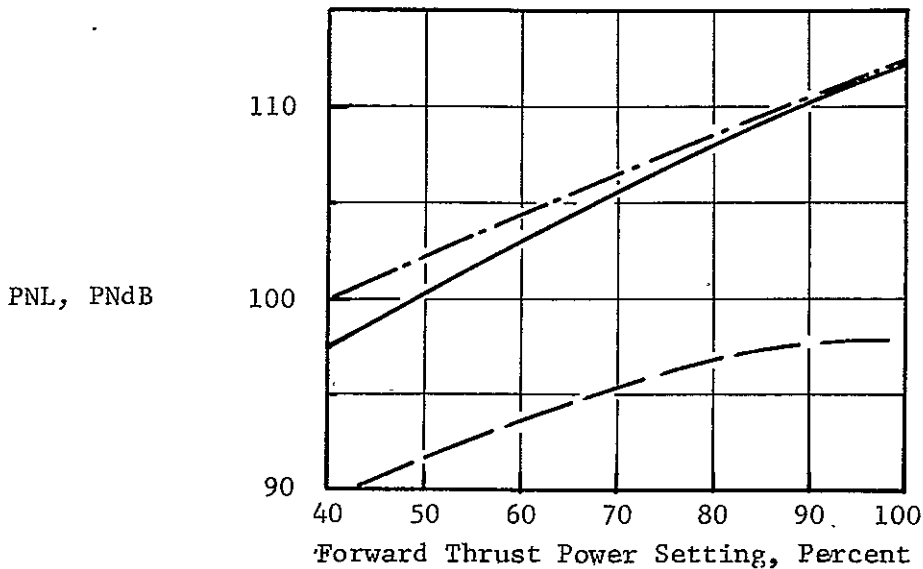
$$P = 3.0 \text{ m.}$$

$$\beta = 45^\circ$$

$$\frac{A_{290}}{A_{T/O}} = \begin{cases} 1.146 & \text{(Baseli)} \\ 1.52 & \text{(Open)} \end{cases}$$

- Open Duct
 - - - Baseline Duct
 - · - Engine Noise
- } Thrust Reverser Noise

• 1.38 Fan Pressure Ratio Cycle



Geometric Parameters

$$L_c = 1.245 \text{ m.}$$

$$P = 2.884 \text{ m.}$$

$$\beta = 45^\circ$$

$$\frac{A_{290}}{A_{T/O}} = \begin{cases} 1.22 & \text{(Baselin)} \\ 1.62 & \text{(Open)} \end{cases}$$

Figure 16 Cascade Reverse Thrust Noise.

Geometric Parameters

Fan Pressure Ratio	1.34	1.38
L_c	1.295 m.	1.245 m.
P	3.0 m.	2.884 m.
β	45°	45°
$A_{290}/A_{T/O}$	$\begin{cases} 1.146 \text{ (Baseline)} \\ 1.52 \text{ (Open)} \end{cases}$	$\begin{cases} 1.22 \text{ (Baseline)} \\ 1.62 \text{ (Open)} \end{cases}$

- 152.4m. (500 ft.) Sideline
- 4 Engines

— Open Duct
 - - - Baseline Duct

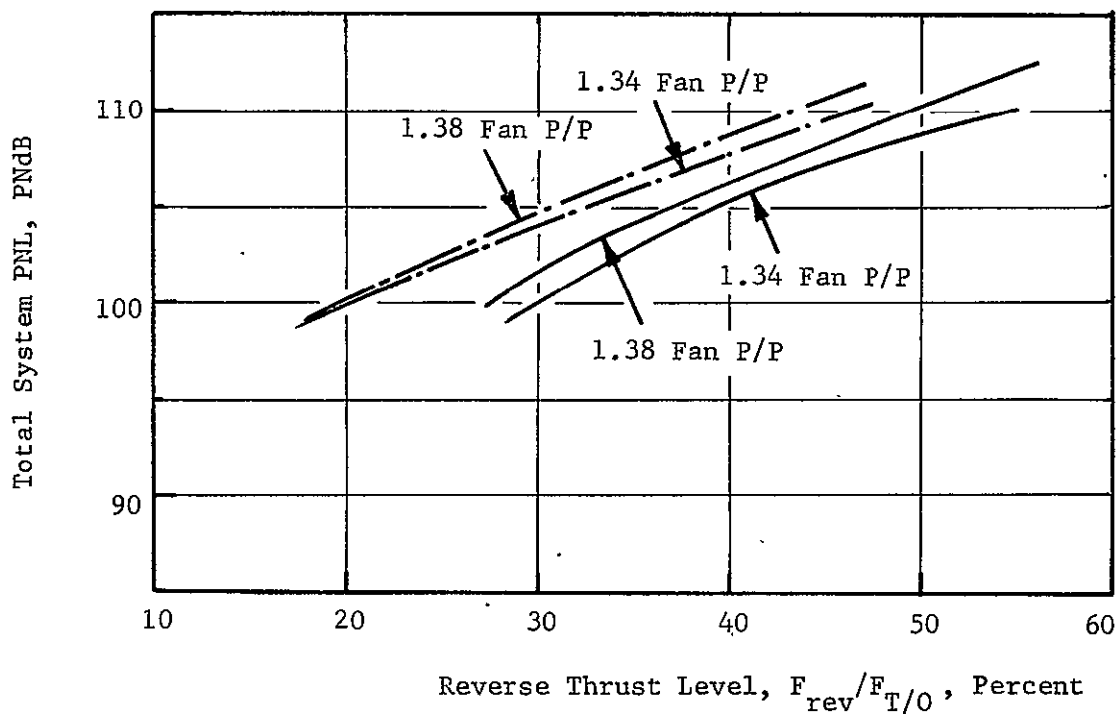


Figure 17 Total System Reverse Thrust Noise with Cascade.

- 152.4 m. (500 ft.) Sideline
- 4 Engines
- 20 Percent Thrust, $F_{rev}/F_{T/O}$
- 1.38 Fan Pressure Ratio Cycle, Baseline Duct

Geometric Parameters

$\beta = 45^\circ$ $L_c \approx 1.245$ m.
 $P = 2.884$ m. $A_{290}/A_{T/O} = 1.22$

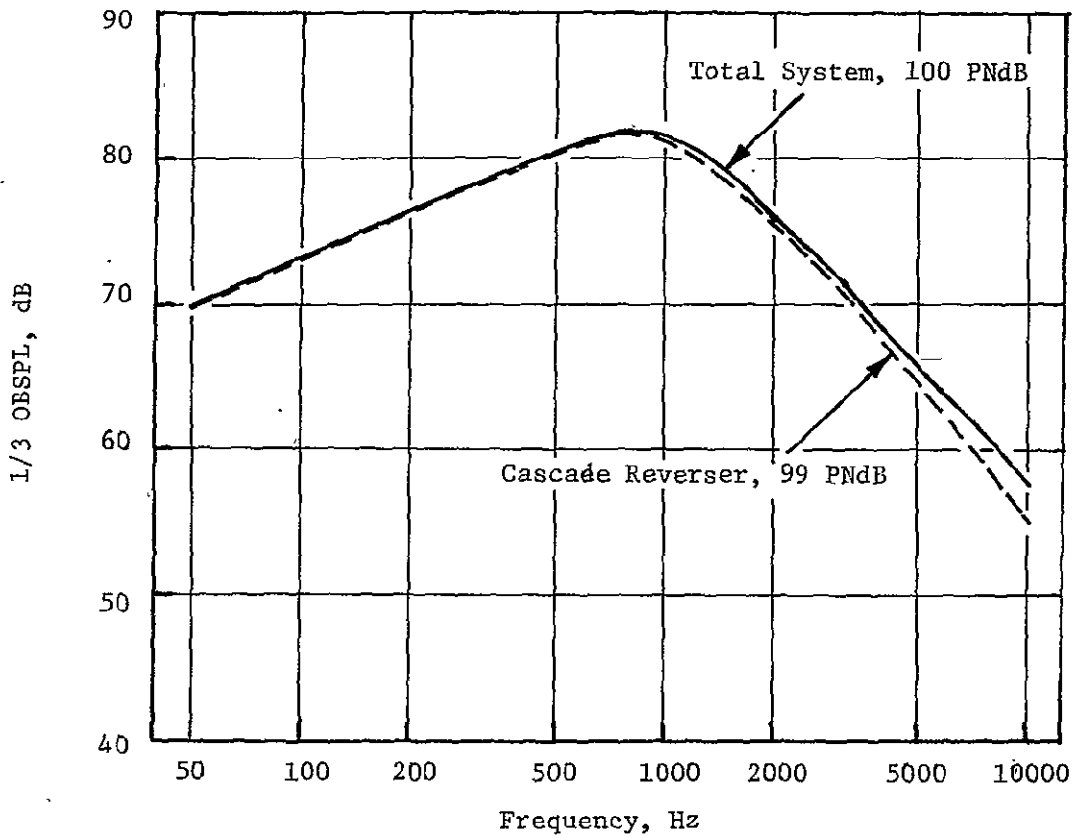


Figure 18. Cascade Reverse Thrust Spectra.

3.6.3 Post Exit Target Reverser Integral With Wing

The increased complexity and function of exhaust nozzles designed for commercial OTW STOL transport application has made thrust reverser design and integration into the nacelle a more difficult task. Therefore, an alternative approach to reverser design for these complex systems was investigated during this study program to determine whether or not a simpler concept could be found. The post exit target reverser concept shown in Figure 19 evolved from this study. The concept employs a single blocker door and attached side skirts positioned aft of the exhaust nozzle. In forward flight the blocker and skirt assembly is stowed in the wing and forms a portion of the wing upper surface. During thrust reversal a single actuator attached to the front spar rotates the blocker door upward to block the exhaust flow and direct it into the lip region where final exhaust flow turning is accomplished. The lip geometry is fixed as shown, with the assumption that during the initial phase of reverser deployment, the lip area blockage in the nozzle exit plane is compensated for by opening the nozzle side doors to a larger area by the engine control system. (As an alternate, an articulated lip could be employed with some increase in spacing required between the nozzle exit and blocker hinge). The reverser side skirts are used to control lateral flow spreading. These skirts rotate forward simultaneously with blocker door actuation through an appropriate linkage and bellcrank arrangement. As shown in Figures 19 and 20, the combined width of the blocker door and side skirts is significantly greater than the open nozzle width. This configuration provides a target geometry capable of capturing the spreading exhaust flow for good reverse thrust performance.

Estimated reverse thrust characteristics for this concept is given on Figure 20. The carpet plot presented on this figure shows the effects of blocker door height and width on reverse thrust for a fixed blocker door angle of 20° and a lip height ratio of 0.20. The performance matrix was derived from data presented in Reference 13 and derated 15% (assumed risk factor) to compensate for the unique D nozzle efflux spreading characteristic of this application. As shown on Figure 20 and the accompanying

Bell Crank
and Linkage

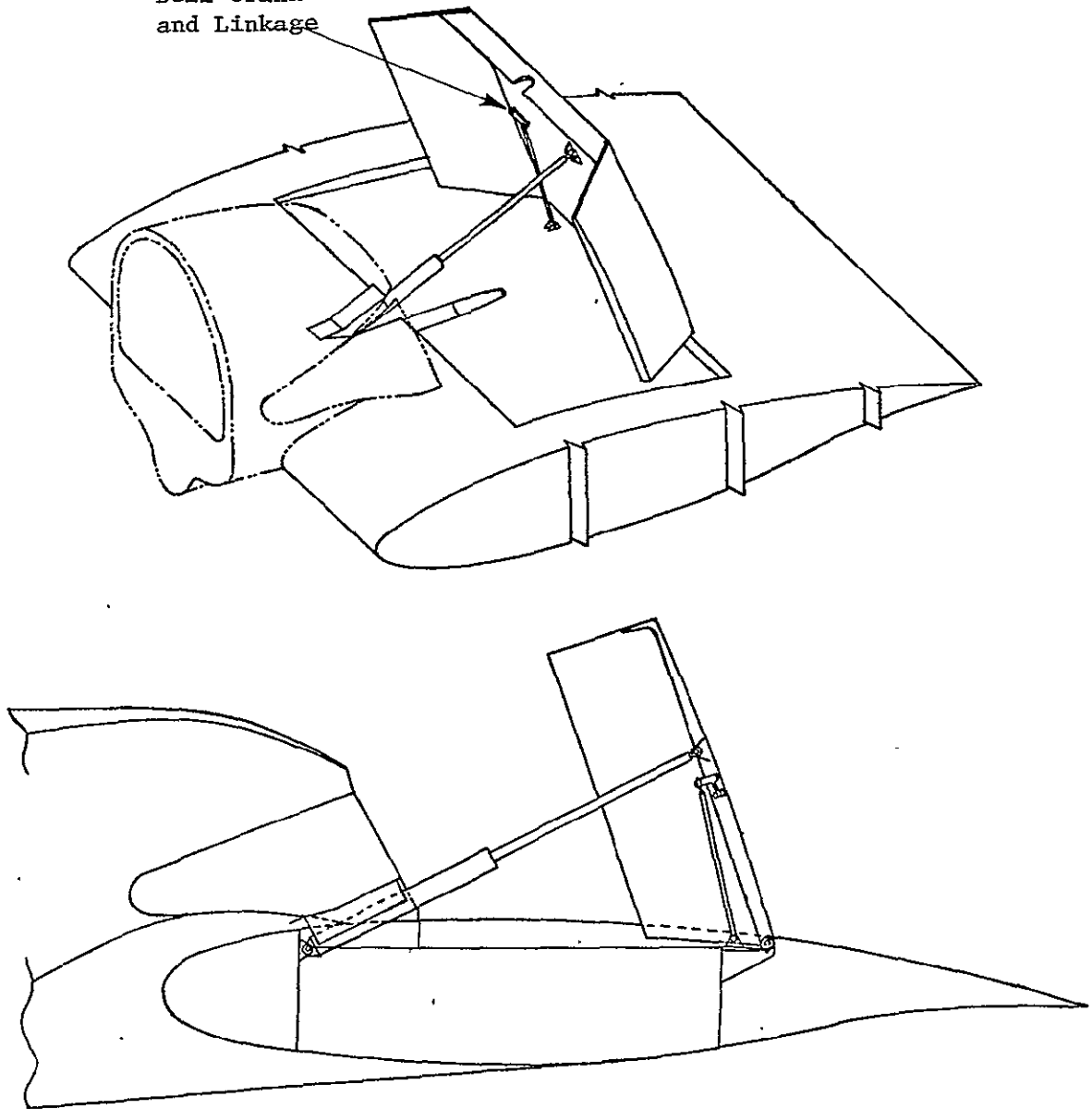
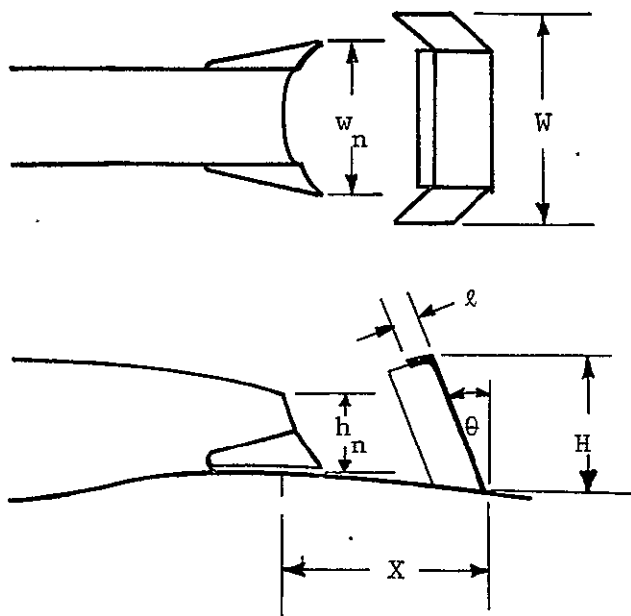


Figure 19 Post Exit Target Reverser.



Selected Geometry

$$X/h_n = 2.7$$

$$H/h_n = 1.96$$

$$\ell/h_n = .21$$

$$W/w_n = 1.4$$

$$\theta = 20^\circ$$

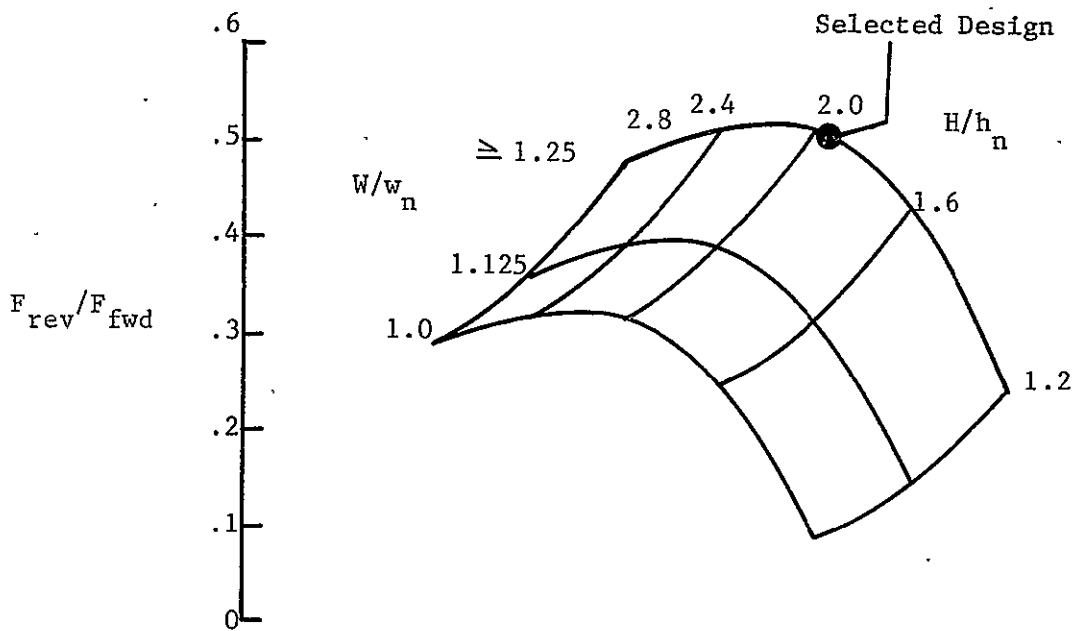


Figure 20 Post Exit Target Reverser Performance.

tabulation of geometric characteristics, this concept can meet the 50% thrust reversal objectives of this study.

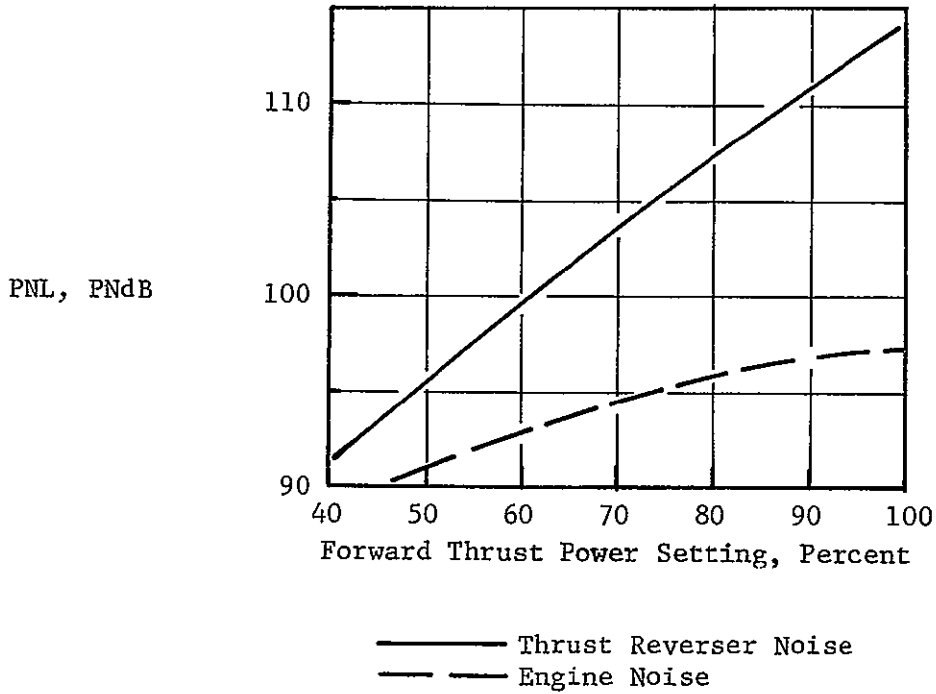
Application of this concept to the OTW STOL transport will require a change in current wing structural design philosophy with local reduction in spar depth and relocation of wing stress panels beneath the reverser. The wing chord selected for the installation shown on Figure 19, is representative of the inboard nacelle location of the transport configuration given in Figure 3. Considering reverser envelope requirements and propulsive lift flap stowage needs, some change in wing planform design may also be necessary, with utilization of a long chord untapered geometry in the propulsive lift section to accommodate outboard nacelle/reverser installation. The post exit reverser concept does not adversely affect nacelle performance.

The post exit target was evaluated acoustically using the same data base as that for the integral target configurations, Section 3.6.1. Two differences were account for. The first being the charging station which for the post exit target is the forward thrust nozzle exit plane and the second being an increased spacing between the charging station and the target. The post exit target is 2.7 nozzle heights downstream of the exit plane while the integral nozzle has only 1.1 heights separation. With the takeoff nozzle area as a reference, the velocity entering the post exit target is relatively high. This higher velocity is offset by the increased spacing which was found to decrease noise by $30\log[(x/h_n)/(x/h_n)_{ref}]$. The resultant post exit reverser noise is shown in Figure 21 as a function of engine power setting. As with Sections 3.6.1 and 3.6.2 this noise was combined with the engine noise to obtain total system noise. These levels are shown on Figure 22 relative to the reverser thrust level. The higher pressure ratio cycle is louder due to the higher nozzle velocities. The 100 PNdB goal can be met at 28% reverse thrust with the 1.38 fan pressure ratio cycle.

The post exit target is higher in frequency than the integral target because of the increased charging station velocity. Figure 23 shows an estimated spectrum for 28% reverse thrust that peaks at 200 Hertz. This

- 152.4m. (500 ft.) Sideline
- 4 Engines

• 1.34 Fan Pressure Ratio Cycle



• 1.38 Fan Pressure Ratio Cycle

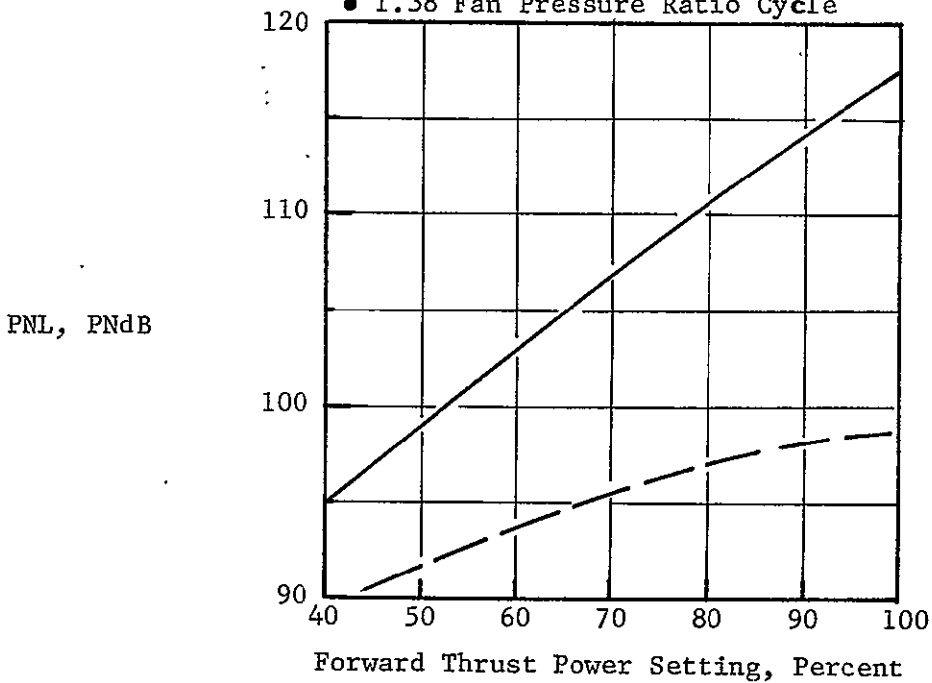


Figure 21 Post Exit Target Reverse Thrust Noise.

- 152.4m. (500 ft.) Sideline
- 4 Engines

Geometric Parameters

$$X/h_n = 2.7 \quad l/h_n = 0.21$$

$$H/h_n = 1.96 \quad W/w_n = 1.4$$

$$\theta = 20^\circ$$

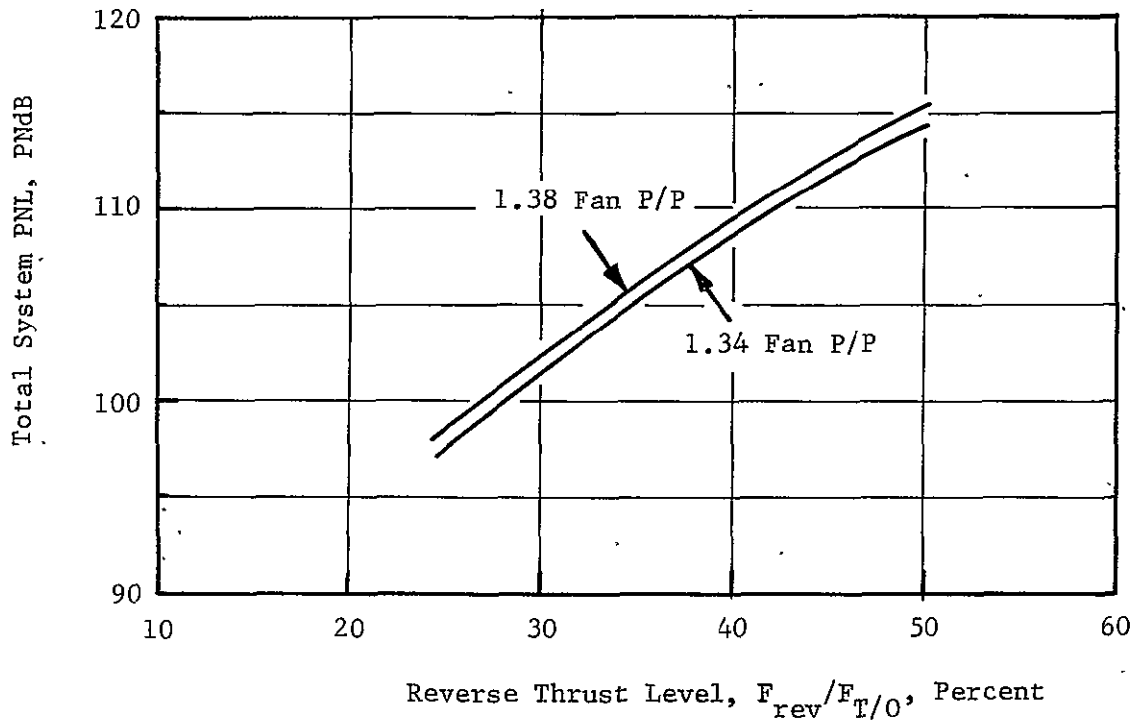


Figure 22 Total System Reverse Thrust Noise with Post Exit Target.

- 152.4 m. (500 ft.) Sideline
- 4 Engines
- 28 Percent Thrust, $F_{rev}/F_{T/0}$
- 1.34 Fan Pressure Ratio Cycle, Baseline Duct

Geometric Parameters

$$X/h_n = 2.7 \quad \ell/h_n = 0.21$$

$$H/h_n = 1.96 \quad W/w_n = 1.4$$

$$\theta = 20^\circ$$

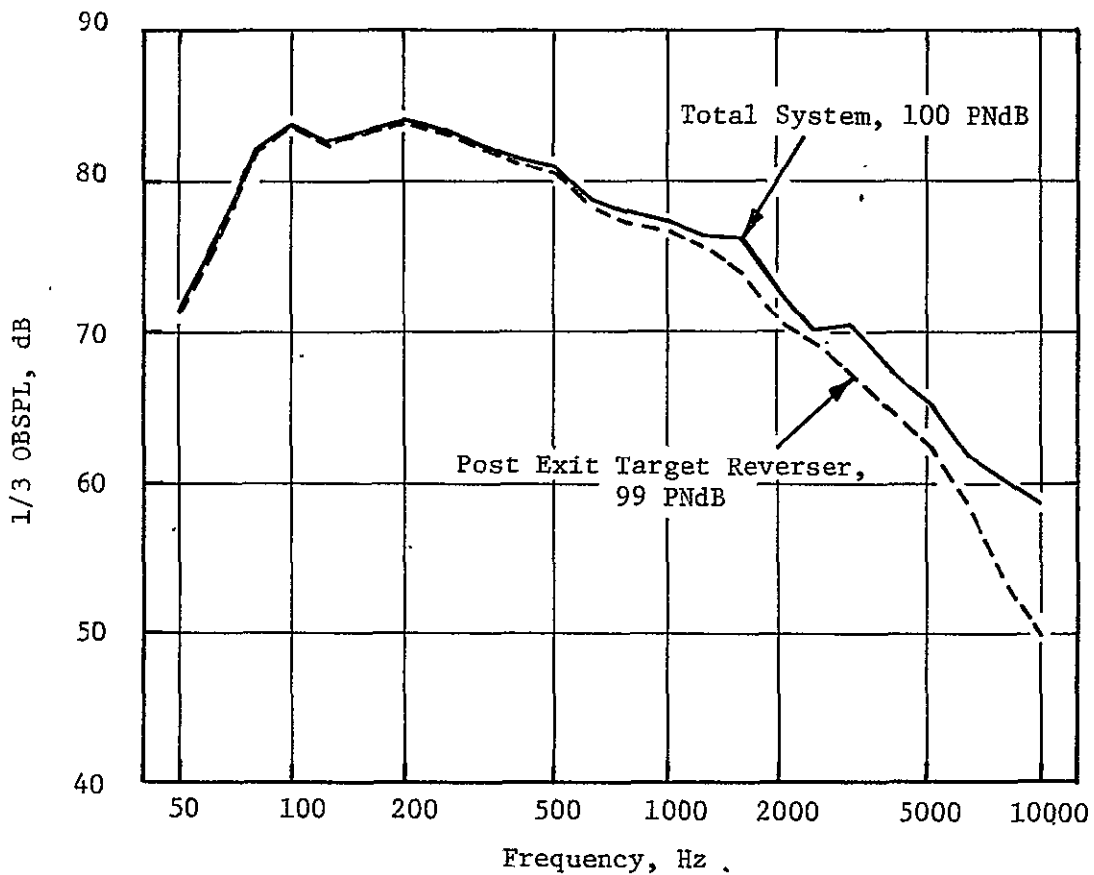


Figure 23. Post Exit Target Reverse Thrust Spectra.

would offer a slight advantage over the integral target in controlling interior cabin noise levels.

3.6.4 Effect of Aircraft Size

Since the acoustic goal of 100 PNdB is independent of aircraft gross weight the effects of aircraft size were evaluated for the baseline duct, high pressure ratio cycle, cascade reverser configuration. This design met the 100 PNdB goal at 20% estimated reverse thrust. Cycle data at this point was scaled to engine sizes corresponding to 43,356 kg (100,000 lb), 90,712 kg (200,000 lb) and 113,391 kg (250,000 lb), aircraft gross weight at a constant thrust to weight ratio of 0.6. Fan noise and reverser noise were scaled spectrally to account for changes in engine size when calculating PNdB. A 10 log (thrust) factor was applied to each size to account for growth. Results of the calculations are shown in Figure 24. Between 61,235 kg (135,000 lb) and 113,391 kg (250,000 lb) there is a 1.5 PNdB increase in total system noise. Thus the higher gross weight aircraft would have to operate below 20% reverse thrust. From the shape of Figure 17, it is estimated that the 113,391 kg (250,000 lb) aircraft would meet 100 PNdB at 17% reverse thrust. For gross weights between 61,235 kg (135,000 lb) and 45,356 kg (100,000 lb) there is essentially no change in total system noise. Over this range the benefit of smaller engines is offset by the higher frequency and increased PNdB weighting.

Aircraft size does not affect engine nacelle or reverser aerodynamic design. Within the ground rules established for the aircraft configuration and thrust to weight ratio, landing distance calculations are also valid.

3.7 CONCEPT SELECTION FOR MODEL DESIGN (TASK II)

Results of the aerodynamic and acoustic analysis, Sections 3.5 and 3.6, have shown that all three concepts can meet the stopping distance requirements for short operational landing field length and that only one of these concepts, the integral nozzle target reverse penalized cruise performance. It was shown further that these high performance thrust

- 152.4m. (500 ft.) Sideline
- 4 Engines
- Thrust/Weight = .6
- 20% Reverse Thrust ($F_{rev}/F_{T/O}$)
- 1.38 Fan Pressure Ratio

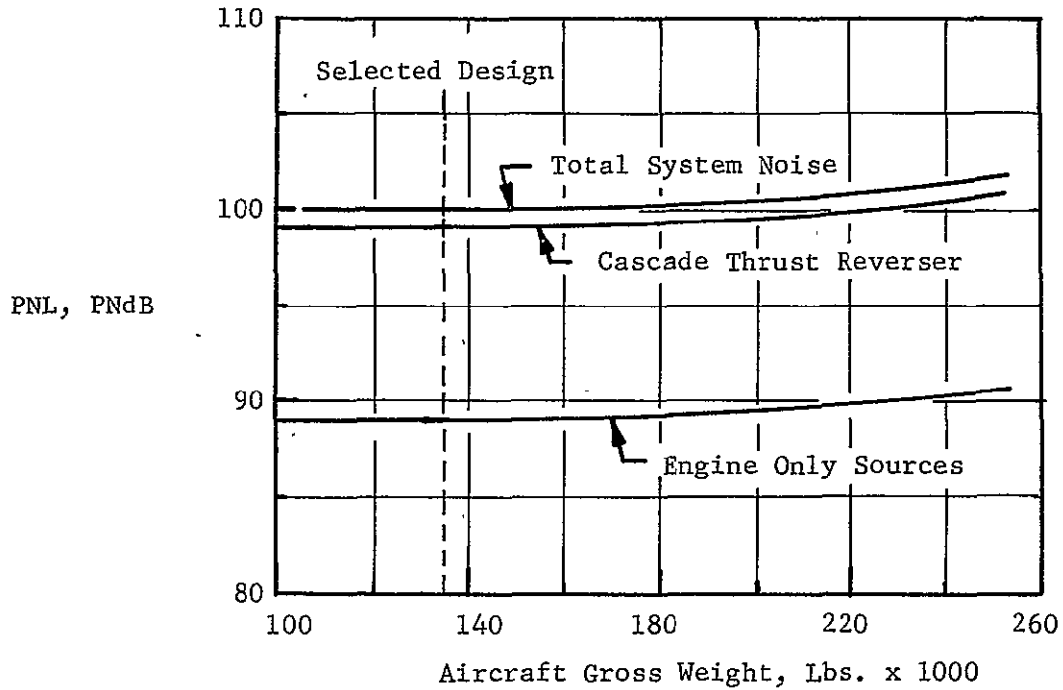


Figure 24 Effect of Aircraft Gross Weight on Reverse Thrust Noise.

reversers provided sufficient stopping capability to allow their operation within the noise goal.

Table II summarizes the estimated maximum reverse thrust obtainable for each reverser concept within the limit of 100 PNdB on a 152.4 m (500 ft) sideline. With the baseline duct and either cycle, the post exit target can be operated at slightly more thrust than either the cascade or integral target type. The reasons for the post exit target being quieter are that the duct baseline duct results in velocities entering both the integral type target and cascade that are relatively high and correspondingly noisy while the post exit target benefits from the large spacing between the nozzle and target. For the open duct configuration the integral type target is best with the post exit target the worst. This is the result of lowered duct velocities which help both the integral target and cascade but have no effect on the post exit target. It is possible to stop the aircraft with any of the reverse thrust levels shown on Table II.

Spectrally the cascade reverser has an advantage for interior noise considerations. With the baseline duct, the cascade peaks at a higher frequency than either the integral target or the post exit target. A quantitative evaluation of the internal noise benefit was beyond the scope of the program. However, all other things being equal, the cascade reverser would be preferable.

A qualitative assessment of the mechanical aspects of the designs was also made. These data are presented on Table III along with the aero/acoustic findings. From the data presented, the top arc cascade reverser concept was selected as the most attractive system, being mechanically the simplest and lightest with lowest potential manufacturing cost. When used with the higher fan pressure ratio cycle (1.38), this propulsion system provides the best installed aerodynamic configuration.

Estimated aero/acoustic performance and significant geometric parameters for the selected top arc cascade reverser are summarized in Table IV.

Table II

Summary of Reverse Thrust Obtainable within Noise Goal Limit.

<u>Configuration</u>	<u>Ratio of Reverse Thrust to Takeoff Forward Thrust that Results in 100 PNdB on a 152.4m. (500 ft.) Sideline.</u>		
	<u>Integral Target</u>	<u>Cascade</u>	<u>Post Exit Target</u>
1. Baseline Duct 1.34 Fan P/P Cycle	22.5%	20.5%	28.0%
2. Baseline Duct 1.38 Fan P/P Cycle	22.5%	20.0%	27.0%
3. Open Duct 1.34 Fan P/P Cycle	40.5%	30.0%	28.0%
4. Open Duct 1.38 Fan P/P Cycle	43.0%	27.5%	27.0%

Table III
OTW STOL Transport Reverser Concept Comparison

	QCSEE Target	Reverser Type	
		Top Arc Cascade	Post Exit Target
Reverse Thrust Performance Objectives Met	Yes	Yes	Yes
Meets Engine Cycle Area Requirements	Yes	Yes	Yes
Stopping Distance Requirement Met at 100 PNdB	Yes	Yes	Yes
Relative Cruise Drag Penalty	2-3% (of Net Thrust)	0	0
Mechanical Simplicity	Most Complex	Simplest	Intermediate Complexity
Relative Weight	Intermediate	Lightest	Heaviest (No Shared Structure)
Aircraft Mechanical Integration	No Problem	No Problem	New Wing Structural Design Concept Involved
Relative Estimated Manufacturing Cost	Intermediate	Least Expensive	Most Expensive (Including Wing Technology)

Table IV

Top Arc Cascade Reverser Geometry and Performance Parameters.

Nacelle Maximum Diameter	1.82 m. (71.65 in.)
Cascade Efflux Angle, β	45°
Cascade Length, L_c	1.245 m. (48.96 in.)
Cascade Wrap Distance, P	2.884 m. (113.55 in.)
Percentage of Cascade Boxes Skewed at 35°	28%
Reverser Estimated Effectiveness, F_{rev}/F_{fwd}	0.51
Percent Estimated Reverse Thrust, $F_{rev}/F_{T/O}$ at 100 PNdB	20%

4.0 APPLICATION OF REVERSER CONCEPT TO SCALE MODEL DESIGN (TASK II)

4.1 SCALE MODEL DUCT DESIGN

The top arc cascade thrust reverser concept will be evaluated at NASA-Ames in the static test facility shown in Figure 25. Because this facility is a single airflow facility, the scale model for the OTW mixed flow nozzle conceptual flowpath was modified by fairing over the core nozzle region. The modified configuration is shown in Figure 26. The centerbody geometry was selected to maintain the same fan plus core engine combined duct area distribution as the mixed flow engine configuration in Figure 13. The cross-sectional area distribution is shown on Figure 27. The exhaust duct cross-sectional geometry for the scale model design is an exact representation of the conceptual engine flowpath, having been photographically reduced to model size directly from the undimensioned engine lines. Forward of engine and scale model station 262, the model flowpath transitions into a cylindrical annular duct with the outer diameter sized to match a facility mounting flange inside diameter of 0.3 meter (11.75 in.). The centerbody cylindrical diameter is 14.148 cm (5.57 in.). The centerbody nose fairing and a means of centerbody attachment to the outer duct has been left for the model detail design phase. The scale model D shaped nozzle exit area for the cruise position is 347.22 cm² (53.82 in.²); the takeoff nozzle area is 423.5 cm² (65.64 in.²) with the variable area side doors set at the position indicated on Figure 26. Comparable full size engine areas for the 1.38 fan pressure ratio, 90,296 newtons (20,300 lb) thrust cycle are 1.353 m² (2097 in.²) and 2.233 m² (2558 in.²) respectively, which converts to a scale model linear scale factor of 16% of full scale.

General Electric undimensioned drawing 4013237-461 (sheets 1 through 14) defines the basic scale model forward thrust flowpath and model station cuts.

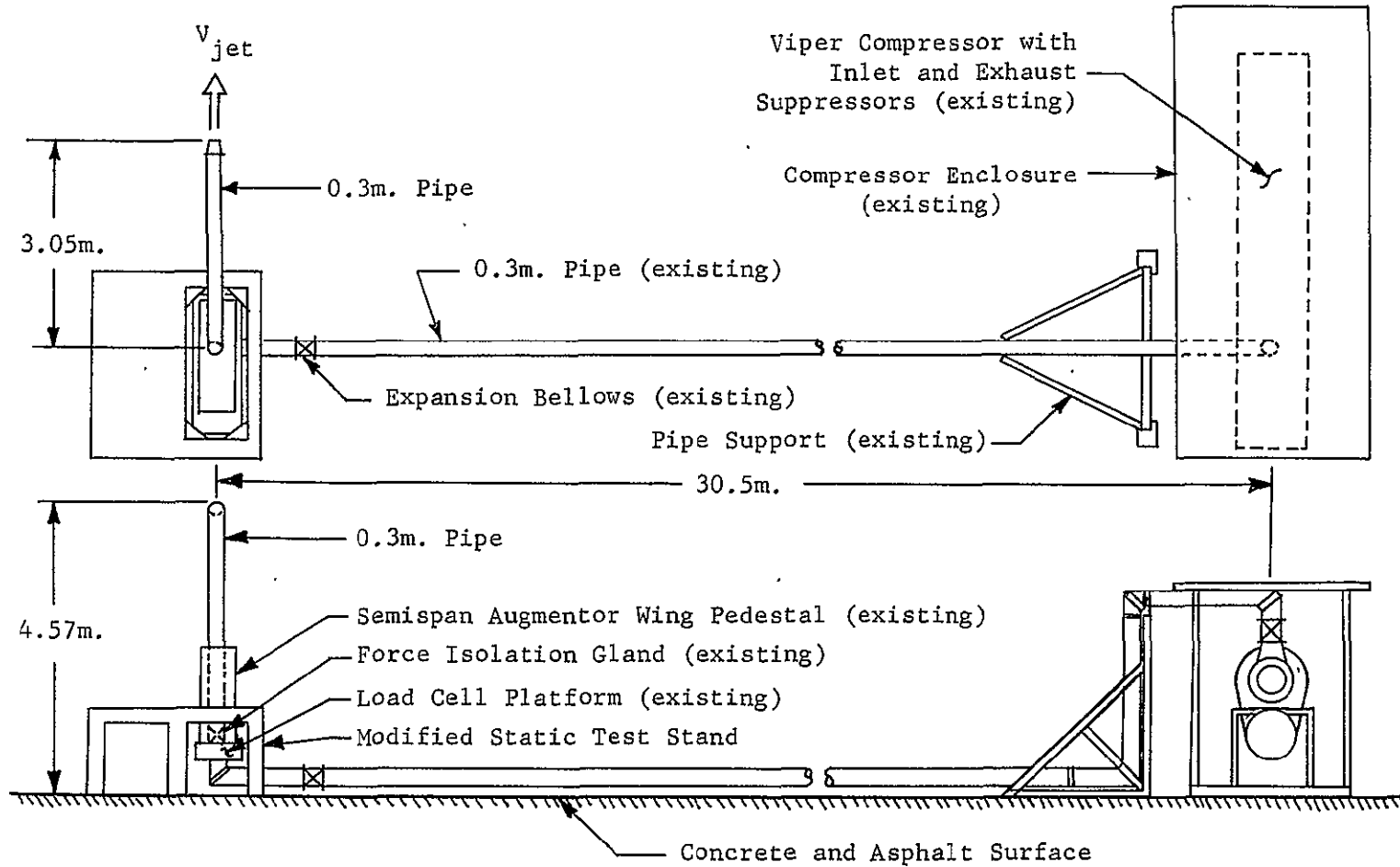


Figure 25 NASA Ames Static Test Facility Schematic.

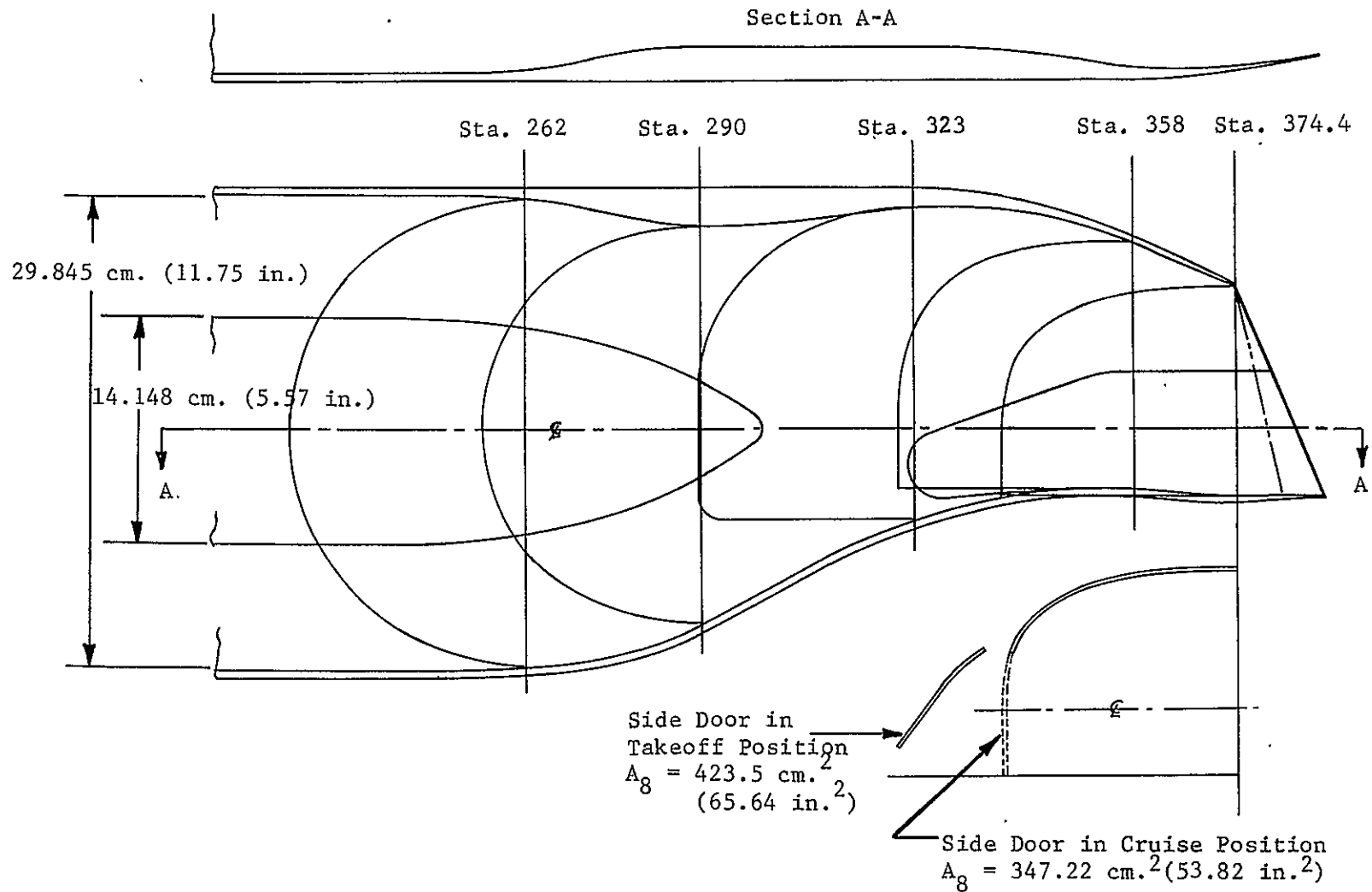


Figure 26 Scale Model Forward Flowpath Design.

• $A_{\text{cruise}} = 347.22 \text{ cm.}^2 (53.82 \text{ in.}^2)$

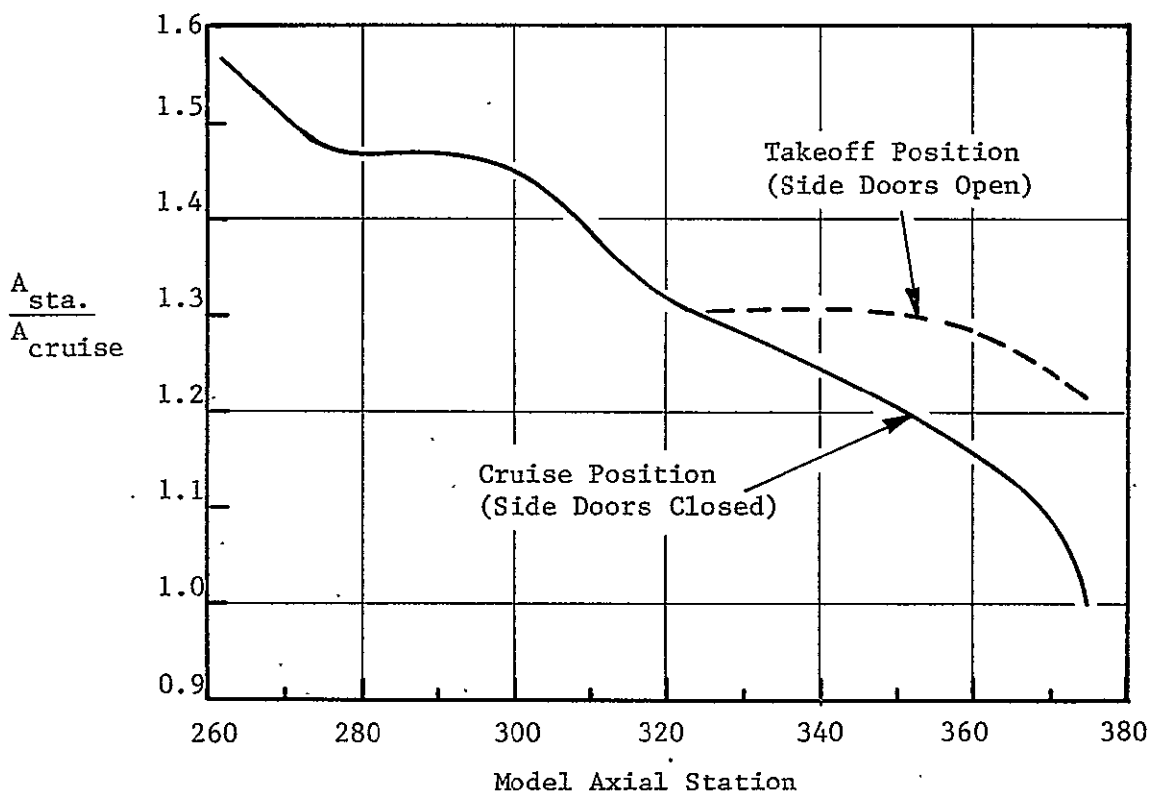


Figure 27 Scale Model Exhaust Duct Cross-Sectional Area Distribution.

4.2 SCALE MODEL REVERSER DESIGN

4.2.1 Aerodynamic Flowpath

The scale model reverser flowpath design is shown on Figure 28. Undimensioned flow lines were developed in scale model size using the same photographic reduction technique employed for the forward thrust configuration. Model station cross-sections are the same as the forward mode position with appropriate stations translated aft to the full reverse position. Nonessential duct geometry aft of the blocker door was cut off. The blocker door shape and axial position within the duct matches the nacelle conceptual reverser flowpath of Figure 13. For simplicity of design, reverser tee track and actuator blockages were not simulated in the model. The reverse cascade section shown on Figure 28 is cylindrical in cross section, having an exit diameter of 16.03 cm (6.31 in.) and a length of 19.99 cm (7.87 in.); circumferential extent is 172°. The cascade roll out view shows a seven sector arrangement with each sector simulating two cascade box positions in the full scale conceptual design. Two of the scale model sectors (28% of total) are skewed upward at a 35° angle to provide a representative aircraft reverser efflux pattern. The total cascade discharge geometric area is 613.31 cm² (95.06 in.²), as measured across the throats of the cascade vane passages and ignoring cascade sector side rail blockage. With this area the model reverser matches the forward nozzle airflow for the takeoff area setting with sufficient margin to allow for up to 15% of total cascade area for detail design of the cascade boxes and approximately 10% additional area margin for aerodynamic risk. Cascade physical discharge area requirements were established at 490.66 cm² (76.05 in.²) based on total pressure losses and flow coefficient characteristics from Reference 9.

General Electric folder series drawing 4013237-462 defines the undimensional scale model flowpath and cascade section. Appropriate station cross sections are defined on drawing 4013237-461 (sheets 2 through 14) as discussed in Section 4.1.

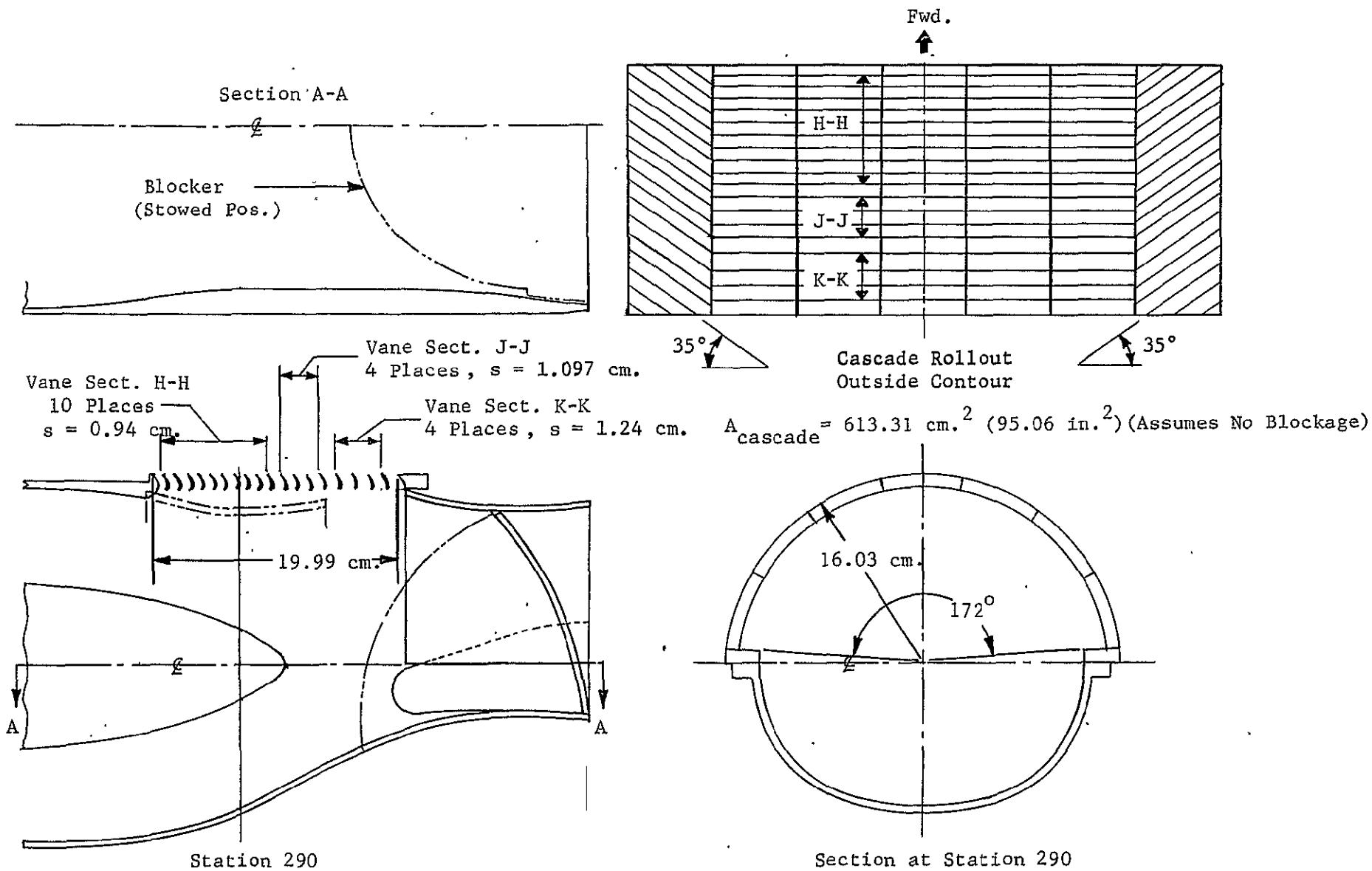


Figure 28 Scale Model Reverser Flowpath Design.

4.2.2 Cascade Vane Design

Flow angles entering the cascade vanes vary considerably along the axial extent of the cascade boxes, with flow angles ranging from about 40° with respect to the engine centerline in the forward section of the box to more or less radial entry in the rearmost region. In order to accommodate this large entry flow angle variation, three groups of vane geometries were selected, consistent with current CTOL reverser design practice. Each group is illustrated on Figure 29. Each vane section is designed to produce a reverse flow exit angle of 45° . For this exit condition the vane camber angle was selected to match approximate entrance flow angles expected in the front half, third quarter and rear quarter of the cascade boxes. As shown, camber angles ranged from 110° up front, 91° in the mid section and 62° in the rear. Vane chord and spacing were selected to provide nominal values of solidities of 1.4, 1.28 and 1.23 front to rear, respectively, to meet overall flow turning angle requirements. Vane chord dimensions shown on Figure 29 were selected to provide a vane radial height of 1.27 cm (0.5 in.) on the model. This height is not a direct scale of the full scale vane geometry (3.81 cm); rather it was selected to facilitate scale model fabrication. The vane cross-sections were defined using the design methods represented in Reference 14. Vane maximum thickness is 15% at 20% of vane chord. For vane manufacturing purposes vane contours were drawn up 20 times full size. These contours are documented on General Electric drawing 4013237-460.

4.3 SCALE MODEL NOISE ESTIMATES

Aerodynamic simulation of the Task I engine flowpath was obtained by maintaining duct Mach number and pressure ratio. However, the model operates at a lower gas temperature than the engine, thus the internal and reverser efflux velocities are lower. As a result, the model will be approximately 1.5 PNdB quieter when scaled to full scale size than the engine estimates presented in Section 3.6.2.

• 45° Discharge Flow Angle, All Sections

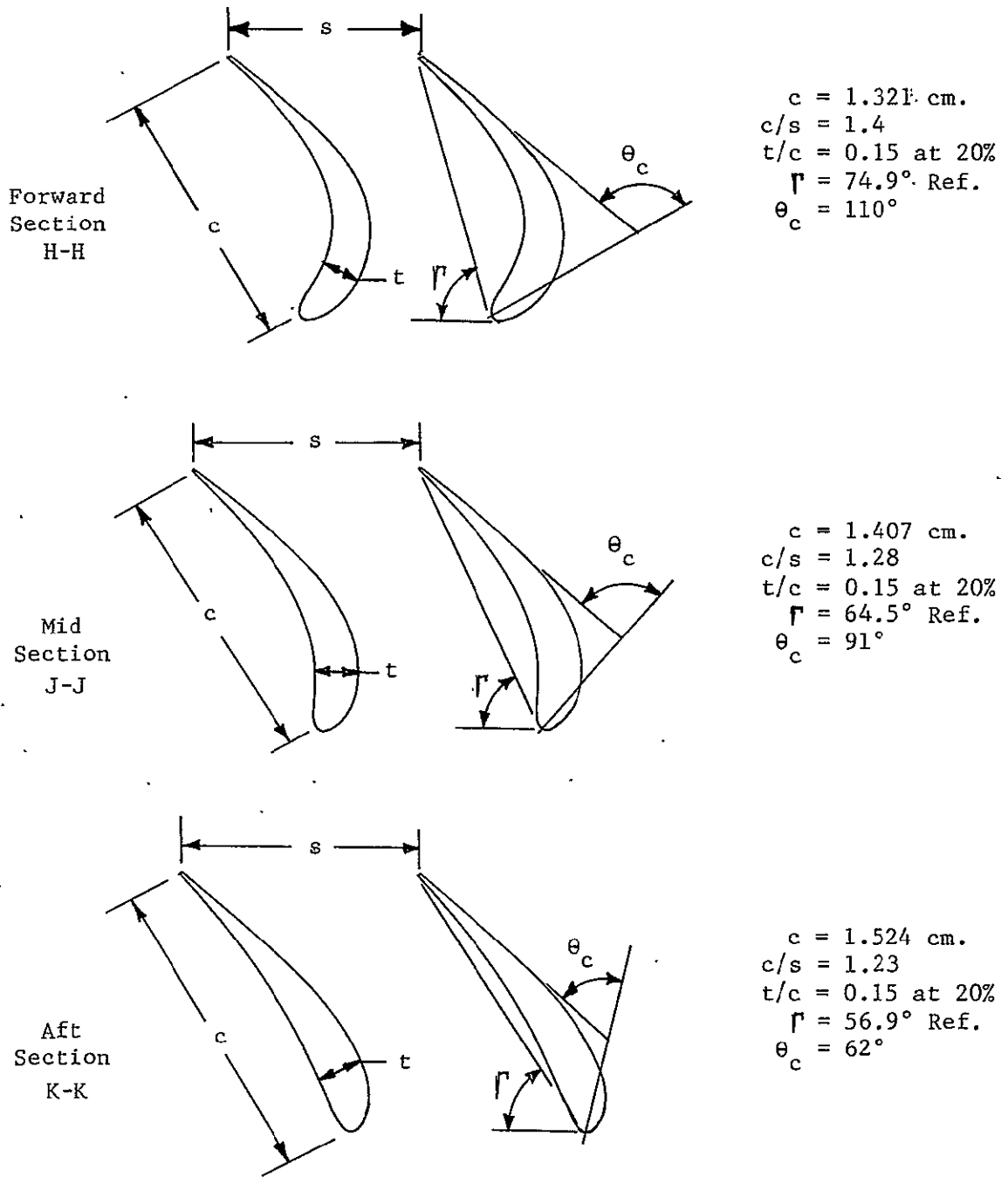


Figure 29 Cascade Vane Geometry.

Estimates of the scale model peak OASPL and spectra were made for comparison with as measured levels after completion of the model tests. These model estimates, shown in Figures 30 and 31, were based on the results of Reference 12 and estimates of the aerodynamic performance with regard to internal and reverser efflux velocities.

● 30.48 m. (100 ft.) Sideline

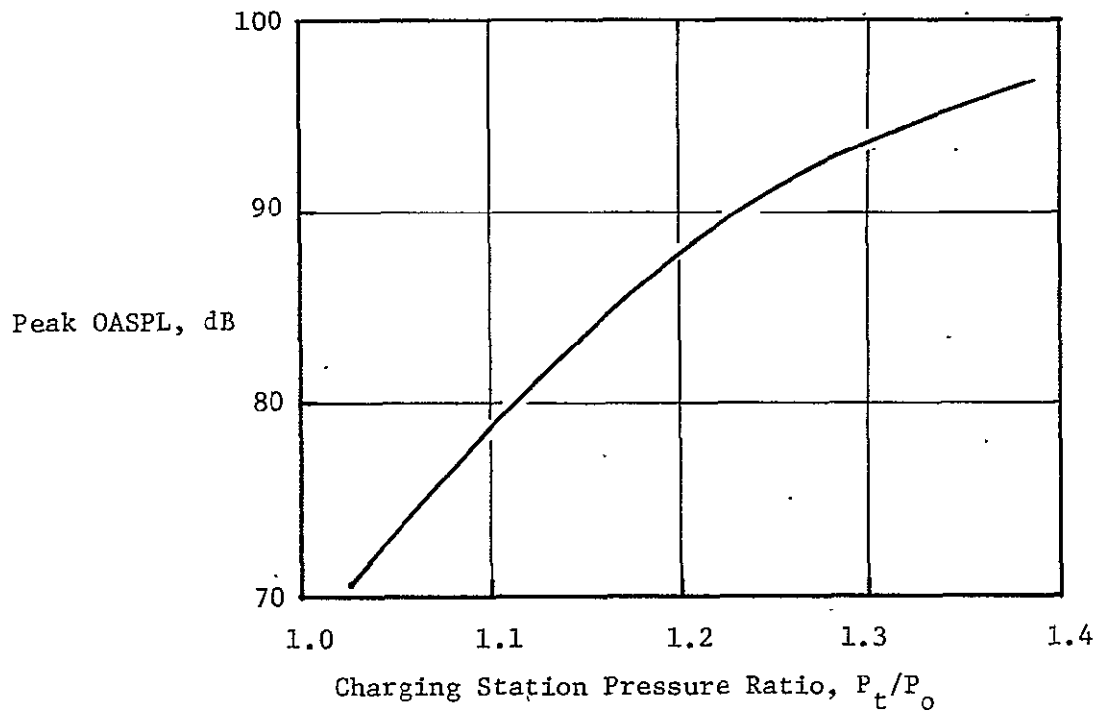


Figure 30. Predicted Scale Model Cascade Reverse Thrust OASPL.

- 30.48 m. (100 ft.) Sideline
- Peak OASPL Angle
- 1.34 Charging Station Pressure Ratio, (P_{t290}/P_o)

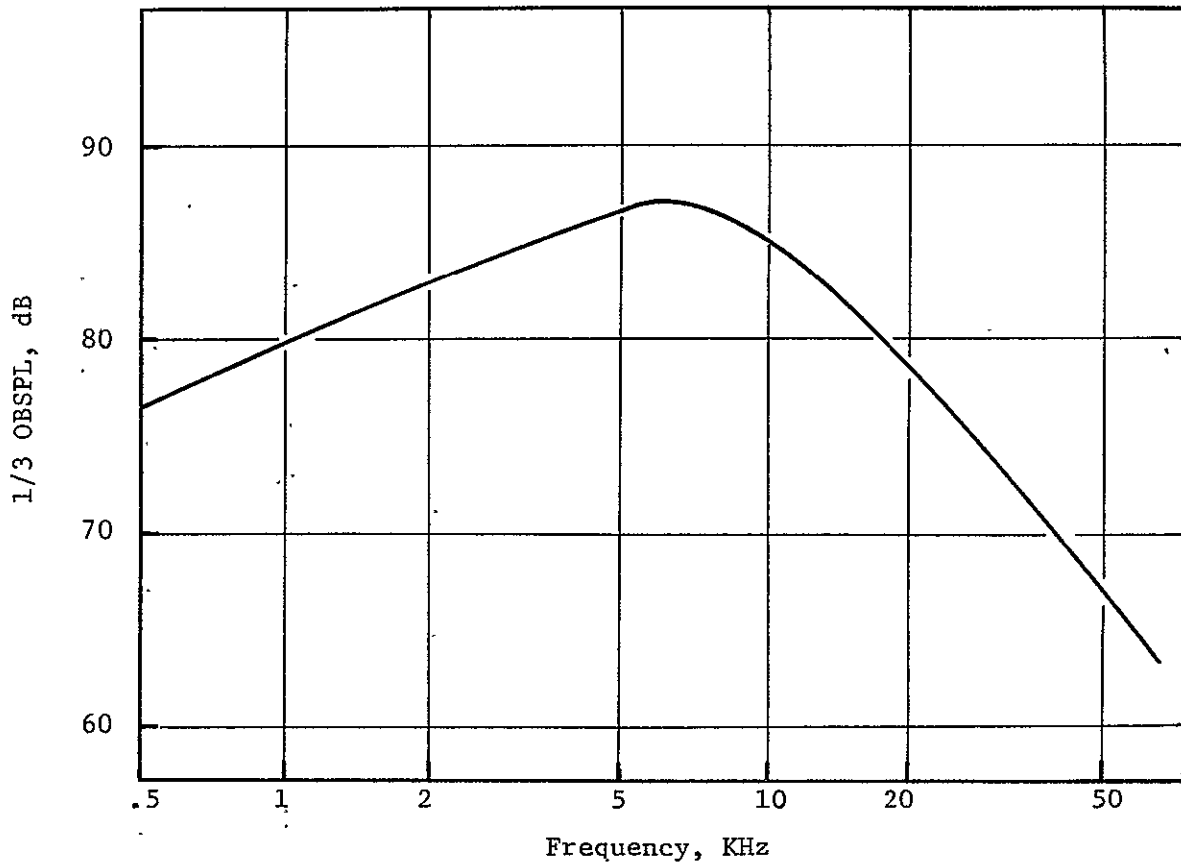


Figure 31. Predicted Scale Model Cascade Thrust Reverser Spectra.

5.0 NOMENCLATURE

A_{cruise}	Nozzle exit area at cruise	cm^2
A_{sta}	Duct cross-sectional area at given station	cm^2
$A_{T/O}$	Nozzle exit area at takeoff	cm^2
A_8	Core exhaust nozzle exit area	cm^2
A_{290}	Duct cross-sectional area at station 290	cm^2
C	Wing chord	meters
C_r	Chord at wing root	meters
c	Cascade vane chord	cm
C_d	Airplane drag coefficient	-
C_l	Wing lift coefficient	-
D_{th}	Target reverser charging station height	meters
D_{max}	Maximum nacelle diameter	meters
EPNL	Effective perceived noise level	EPNdB
F_{fwd}	Forward thrust	newtons
F_N	Engine net thrust at flight condition	newtons
F_{rev}	Reverse thrust	newtons
$F_{T/O}$	Takeoff gross thrust	newtons
H	Blocker door height	meters
h_n	D nozzle height	cm
HZ	Frequency	cycles/sec
L	Target reverser lip length	meters
L_c	Cascade box length	meters, cm
l	Lip length, post exit target reverser	meters
1/3 OBSPL	1/3 Octave band sound pressure level	dB
OASPL	Overall sound pressure level	dB
P	Cascade wrap distance	meters
P_t	Total pressure	newtons/ m^2
P_o	Ambient pressure	newtons/ m^2
PNL	Perceived noise level	PNdB
S	Wing semi-span	meters
S_w	Wing area	m^2

s	Cascade spacing	cm
t	Cascade vane maximum thickness	cm
V_{cutoff}	Aircraft velocity for throttle retard in reverse	m/s
W	Post exit target width	meters
W_c	Target reverser charging station width	meters
W_{fwd}	Forward thrust airflow	kg/sec
W_{rev}	Reverse thrust airflow	kg/sec
w_n	D Nozzle width at takeoff	meters
X	Reverse blocker spacing	meters
α	Cascade vane skew angle	degrees
β	Lip angle, cascade discharge angle	degrees
β_e	Reverser effective efflux angle	degrees
Γ	Cascade vane stagger angle	degrees
Δ	Change in parameter indicated	-
θ	Blocker angle	degrees
θ_c	Cascade vane camber angle	degrees

6.0 REFERENCES

1. "Quiet Propulsive Lift Research Aircraft Design Study," Boeing Commercial Airplane Company, NASA CR-137557.
2. Rabone, G.R., et al, "QCSEE Task I - Parametric Study," General Electric/NASA Contractor Report, April 1973.
3. Neitzel, R., et al, "QCSEE Task II - Engine and Installation Preliminary Design," General Electric/NASA Contractor Report, June 1973.
4. "QCSEE Task III - Final Report," General Electric/NASA Contractor Report, November 17, 1972.
5. Neitzel, R., et al, "QCSEE Task IV - Effects of Field Length on Propulsion System Selection," General Electric/NASA Contractor Report, January 17, 1973.
6. Cohn, J.A. and Altman, W.A., "Aircraft Landing Distance Computer Program," TM 74-544, General Electric Company.
7. Ammer, R.C. and Kutney, J.T., "Analysis and Documentation of QCSEE (Quiet Clean Short-Haul Experimental Engine) Over-the-Wing Exhaust System," NASA CR-2792, General Electric Company.
8. Stimpert, D.L., "Acoustic and Aerodynamic Results of Tests on a Scale Model Over-the-Wing Thrust Reverser and Forward Thrust Nozzle," General Electric/NASA, R75AEG504, January 1976.
9. Ammer, R.C., "STOL Reverser Scale Model Tests to Determine Effects of Reverser Axial Spacing and Extent of Circumferential Blockage on Performance and Fan Compatibility," General Electric Company, TM 72-437 and TM 72-437-1 (Addendum).
10. Dietrich, Donald A. and Luidens, Roger W., "Experimental Performance of Cascade Thrust Reversers at Forward Velocity," NASA TM X-2665.
11. Kolb, Stephen P., "Developing a Cascade Thrust Reverser," Continental Airlines (Shell Aviation News, November 1976).
12. Gutierrez, D.A. and Stone, J.R., "Results from Cascade Thrust Reverser Noise and Suppression Experiments," AIAA Paper No. 74-46, January 30, 1974.
13. Lewis, W.J., Rolls Royce (1971) Limited and Prechter, H., Motoren-Und Turbinen-Union, "Aerodynamics of Thrust Reverser Design," (publication source unknown).
14. Dunavant, James C. and Erwin, John R., "Investigation of a Related Series of Turbine-Blade Profiles in Cascade," NACA TN 3802.